Assay Setup for High Throughput Screening to Identify Novel Efflux Pump Inhibitors against *Escherichia coli*

Ulla Yrjänheikki
Master Thesis
Discipline of Biopharmaceutics
Faculty of Pharmacy
University of Helsinki
December 2018

HELSINGIN YLIOPISTO
HELSINGFORS UNIVERSITET
UNIVERSITY OF HELSINKI

Tiedekunta/Osasto Fakultet/Sektion – Faculty Faculty of Pharmacy	Osasto/Sektion– Department Division of Pharmaceutical Biosciences	
Tekijä/Författare – Author Ulla Yrjänheikki		
Työn nimi / Arbetets titel – Title Assay Setup for High Throughput Screening to Identify Novel Efflux Pump Inhibitors against *Escherichia coli*		
Oppiaine /Läroämne – Subject Biopharmaceutics		
Työn laji/Arbetets art – Level Master Thesis	Aika/Datum – Month and year December 2018	Sivumäärä/ Sidoantal – Number of pages 68

Tiivistelmä/Referat – Abstract

Background: The World Health Organization (WHO) outlined in their report published in 2014 that antimicrobial resistance (AMR) is a real public health threat worldwide and the actions against it should be taken. Otherwise, the post-antibiotic era where common community-acquired infections can lead to death, could hypothetically become true. The discovery and development of novel antibiotics (ATBs) against Gram-negative bacteria (GNB)-related infections is difficult due to a dual defence mechanism: the extra protection barrier called the outer membrane and efflux pumps which GNB utilize to protect themselves against external noxious compounds. Efflux pumps are expressed at the basal level in GNB, such as *E. coli*, but when exposed to sub-inhibitory concentrations of ATBs and the intrinsic extruding capacity is exceeded, GNB start overexpressing these "so-called" multi-drug resistance (MDR) efflux pumps. The most abundant and studied MDR efflux pump in *E. coli* is a tripartite protein complex AcrAB-TolC which traverse through the bacterial cell envelope and is capable of extruding a broad range of structurally unrelated compounds, thus leading to cross-resistance against several classes of ATBs. It has been suggested that antibacterial activity of existing ATBs could be restored again by inhibiting increased efflux activity through efflux pump inhibitors (EPIs).

Objectives: Define the optimal assay conditions and a positive control (EPI) to be used in high throughput screening (HTS) of novel EPIs. The assay consists of one *E. coli* strain of clinical relevance with high intrinsic efflux activity, one ATB and one EPI, both of them at specific concentrations defined during this study.

Methods: The intrinsic efflux activities of seven *E. coli* strains were studied by Hoechst 33342 (H33342) accumulation assay, both in the absence and presence of five commercially available EPIs. The same assay was used in the dose-response studies in which an optimal concentration of EPIs was identified for further to be utilized in the checkerboard assays. The minimum inhibitory concentrations (MICs) were determined by broth microdilution method according to Clinical and Laboratory Standards Institute. The synergistic effects of ATB and EPI in terms of decreasing the intrinsic MIC value of the ATB were determined in the checkerboard assays partially performed by the Biomek i7 Automated Workstation. The data was analysed by using Microsoft Excel and IBM SPSS Statistics, version 25.

Results and discussion: *E. coli* ATCC 25922 had statistically significantly the highest efflux activity of all wild-type pathogenic and non-pathogenic *E. coli* strains. However, when H33342 accumulation assay was carried out in conjunction with EPIs, *E. coli* BAA1161 (uropathogenic strain) had the highest median increase in the intracellular level of H33342. Mefloquine showed to be the most potent of all EPIs at the tested concentrations. However, mefloquine increased the intracellular H33342 accumulation even in efflux-deficient *E. coli* JW5503 (ΔtolC), thus possible additional modes of action or inhibitory activity towards other efflux pumps might exist. Dose-response studies carried out in ΔtolC *E. coli* JW5503 suggested that CCCP at 1.25 μg/ml and mefloquine at 0.5 μg/ml were the optimal concentrations. However, for mefloquine, when tested at 0.5 μg/ml, the intracellular level of H33342 was not increased in six remaining *E. coli* strains. Therefore higher concentrations up to ½ MIC were tested in the checkerboard assays. In the antibacterial susceptibility testing, *E. coli* BAA1161 was the only strain showing resistance to tetracycline and piperacillin, resulting in MIC ratios (MIC wild-type/MIC mutant) of 512 to 2048. Piperacillin and ofloxacin, which showed a MIC ratio of ≥4 in two *E. coli* strains, were chosen to the checkerboard assays in which mefloquine reduced the intrinsic MIC of piperacillin by 16-fold and CCCP by 32-fold in *E. coli* BAA1161.

Conclusions: *E. coli* BAA1161 was chosen to be used as a model strain in HTS due to the highest median increase in intracellular H33342 accumulation and also for being the only strain with resistance towards the ATBs tested. Mefloquine (16 μg/ml) was the EPI of choice for the positive control in HTS because the synergistic effects observed between piperacillin and mefloquine were most probably explained by efflux pump inhibition and not by antibacterial activity of mefloquine itself. Piperacillin (256 μg/ml) was selected to be used as an ATB in HTS because it was the only ATB which was potentiated by the tested EPIs.

Avainsanat – Nyckelord – Keywords
AcrAB-TolC, checkerboard assay, efflux pumps, efflux pump inhibitors, *Escherichia coli*, high throughput screening, Hoechst 33342, minimum inhibitory concentration, multidrug resistance, synergism

Säilytyspaikka – Förvaringställe – Where deposited
Helsinki

Muita tietoja – Övriga uppgifter – Additional information
Supervisors: Päivi Tammela, Heidi Kidron and Cristina Durante Cruz

HELSINGIN YLIOPISTO
HELSINGFORS UNIVERSITET
UNIVERSITY OF HELSINKI

Tiedekunta/Osasto Fakultet/Sektion – Faculty Farmasian tiedekunta	Osasto/Sektion– Department Farmaseuttisten biotieteiden osasto	
Tekijä/Författare – Author Ulla Yrjänheikki		
Työn nimi / Arbetets titel – Title *Escherichia colille* tehokkaiden efluksipumppuinhibiittoreiden tehoseulontamenetelmän optimointi		
Oppiaine /Läroämne – Subject Biofarmasia		
Työn laji/Arbetets art – Level Pro gradu -tutkielma	Aika/Datum – Month and year Joulukuu 2018	Sivumäärä/ Sidoantal – Number of pages 68

Tiivistelmä/Referat – Abstract

Tausta: Maailman terveysjärjestö WHO linjasi vuonna 2014 julkaisemassaan raportissa, että antibioottiresistenssi on todellinen maailmanlaajuinen terveysuhka, jonka vastaiset toimet on käynnistettävä. Uusien antibioottien löytäminen ja kehittäminen Gram-negatiivisten bakteerien aiheuttamiin tulehduksiin on haastavaa, sillä Gram-negatiivisilla bakteereilla on luontainen puolustusmekanismi tappavia vierasaineita vastaan. Gram-negatiivisilla bakteereilla on soluseinärakenteessaan ylimääräinen kalvorakenne (ulkokalvo), joka vaikeuttaa lääkeaineiden kulkeutumista soluseinän läpi. Lisäksi Gram-negatiivisille bakteereille, kuten *E. colille*, on ominaista efluksipumput, joiden yli-ilmentäminen soluseinärakenteessa on seuraus efluksipumppujen pumppauskapasiteetin ylittymisestä esimerkiksi bakteereiden altistuessa pitkäjatkoisesti matalille, bakteerikasvua estämättömille antibioottipitoisuuksille. Tutkituin ja runsaimmin *E. colissa* esiintyvä monilääkeresistentti efluksipumppu on kolmiosainen AcrAB-TolC-proteiinikompleksi, joka ulottuu koko soluseinärakenteen läpi, pumpaten solun sisältä solunulkoiseen tilaan laajan kirjon rakenteellisesti toisistaan poikkeavia yhdisteitä, aiheuttaen lopulta ristilääkeaineresistenssiä useammalle eri antibioottiryhmälle. Onkin ehdotettu, että nykyisten antibioottien teho voitaisiin palauttaa yhdistämällä lääkehoitoon efluksipumppuinhibiittori (EPI), jolloin terapeuttinen antibioottipitoisuus voitaisiin solunsisäisesti saavuttaa uudelleen.

Tavoitteet: Tehoseulontamenetelmän koeolosuhteiden ja positiivisen kontrollin määrittäminen uusien EPIen löytämiseksi. Menetelmä koostuu korkean efluksiaktiivisuuden omaavasta *E. coli* -kannasta sekä yhdestä EPIstä ja yhdestä antibiootista, molemmat yksittäisellä pitoisuudella testattuna. Tutkimuksessamme valikoitunut EPI toimii tehoseulontamenetelmän positiivisena kontrollina.

Menetelmät: Seitsemän *E. coli* -kannan efluksiaktiivisuus määritettiin Hoechst 33342 (H33342) -kumuloitumiskokeella, sekä ilman että yhdessä viiden EPIn kanssa. Samaa menetelmää hyödynnettiin annos-vastekokeissa, joissa EPIen optimaalinen annos selvitettiin. Matalin bakteerikasvua estävä lääkeainepitoisuus (MIC-arvo) määritettiin mikrolaimennosmenetelmällä CLSI (Clinical and Laboratory Standards Institute) -ohjeiston mukaisesti. Antibiootin ja EPIn keskinäistä synergismiä ja EPIn kykyä laskea antibiootin MIC-arvoa tutkittiin 96-kuoppalevyllä Biomek i7 -robotiikkaa hyödyntäen. Datan analysoimiseen käytettiin Microsoft Exceliä sekä IBM SPSS Statistics -tilasto-ohjelmaa (versio 25).

Tulokset ja pohdinta: *E. coli* ATCC 25922 -kannalla oli korkein efluksiaktiivisuus kaikista villityypin patogeenisistä ja ei-patogeenisistä *E. coli* -kannoista. H33342-kumuloitumiskoe yhdessä viiden EPIn kanssa kuitenkin osoitti, että uropatogeeninen *E. coli* BAA1161 nosti solunsisäistä H33342:n vakaan tilan pitoisuutta voimakkaimmin. Meflokiini osoittautui potenteimmaksi EPIksi H33342-kumuloitumiskokeeseen valikoituneilla pitoisuuksilla testattuna. Odotusten vastaisesti meflokiini nosti H33342:n vakaan tilan pitoisuutta myös *E. coli* JW5503 -kannassa (ΔtolC). Siten tulos saattaisi viitata siihen, että meflokiini vaikuttaa epäselektiivisesti muillakin tavoin tai vaihtoehtoisesti toimii inhibiittorina useammalle eri efluksipumppualatyypille. Annos-vastekokeet *E. coli* JW5503 -kannalla ehdottivat CCCP:n ja meflokiinin optimaalisiksi annoksiksi 1.25 μg/ml ja 0.5 μg/ml. Meflokiinin annos osoittautui kuitenkin liian matalaksi kuudella muulla *E. coli* -kannalla testattuna ja siten synergiatestiin valikoitiin korkeammat pitoisuudet meflokiinia siten, että kokeessa testattu maksimipitoisuus meflokiiniä oli puolet sen MIC-arvosta. Antibakteerisessa herkkyysmäärityksessä *E. coli* BAA1161 osoittautui ainoaksi resistentiksi kannaksi, ja MIC-suhdeluvut (villityypin MIC/mutantin MIC) tetrasykliinille ja piperasilliinille olivat 512 ja 2048. Piperasilliini ja ofloksasiini, joiden MIC-suhdeluku oli vähintään 4 ainakin kahdella eri *E. coli* -kannalla, valikoituvat lopulta synergiatestiin. Meflokiini laski piperasilliinin MIC-arvoa 16-kertaisesti ja CCCP jopa 32-kertaisesti *E. coli* BAA1161 -kannalla.

Johtopäätökset: *E. coli* BAA1161 valikoitui kannaksi uusien EPIen tehoseulontamenetelmään, koska suurin nousu H33342:n vakaan tilan pitoisuudessa havaittiin *E. coli* BAA1161 -kannalla. Lisäksi *E. coli* BAA1161 oli ainoa kanta, jolla osoitettiin olevan antibioottiresistenssiä, joka vastaavasti saatiin kumoutumaan EPIen vaikutuksesta. Meflokiinin (16 μg/ml) kyky tehostaa piperasilliinin antibakteerista vaikutusta selittyi todennäköisesti efluksipumppuinhibitiolla, ei meflokiinin antibakteerisella teholla. Piperasilliini (256 μg/ml) oli sen sijaan ainoa antibiootti, jonka antibakteerinen teho voimistui meflokiinin ja CCCP:n vaikutuksesta.

Avainsanat – Nyckelord – Keywords
AcrAB-TolC, antibakteerinen herkkyysmääritys, efluksipumput, efluksipumppuinhibiittorit, *Escherichia coli*, Hoechst 33342, matalin bakteerikasvua estävä lääkeainepitoisuus (MIC), monilääkeresistenssi, synergiatesti, tehoseulonta

Säilytyspaikka – Förvaringställe – Where deposited
Helsinki

Muita tietoja – Övriga uppgifter – Additional information
Ohjaajat: Päivi Tammela, Heidi Kidron ja Cristina Durante Cruz

TABLE OF CONTENTS

ABBREVIATIONS

AMR = Antimicrobial resistance

ATB = Antibiotic

CAMHB = Cation-adjusted Mueller-Hinton broth

CCCP = Carbonyl cyanide 3-chlorophenylhydrazone

CFU = Colony forming unit

CIP = Ciprofloxacin

CLSI = Clinical and Laboratory Standards Institute

DBP = Distal binding pocket

DMSO = Dimethyl sulfoxide

EP = Efflux pump

EPI = Efflux pump inhibitor

FIC = Fractional inhibitory concentration

GLASS = Global Antimicrobial Resistance Surveillance System

GNB = Gram-negative bacteria

H33342 = Hoechst 33342

HMMA = High-molecular mass antibiotic

HTS = High throughput screening

IM = Inner membrane

LB = Lysogeny broth

LPS = Lipopolysaccharide

MDR = Multidrug resistance

MF = Modulation factor

MHA = Mueller-Hinton agar

MIC = Minimum inhibitory concentration

NMP = 1-(1-Naphthylmethyl)-piperazine

OD = Optical density

OFX = Ofloxacin

OM = Outer membrane

PAβN = Phenylalanine-arginyl β-naphthylamide

PBP = Proximal binding pocket

PBS = Phosphate-buffered solution

PIP = Piperacillin

PMF = Proton motive force

RND = Resistance nodulation division superfamily

RT-qPCR = Real-time quantitative reverse transcriptase-polymerase chain reaction

SMMA = Small-molecular mass antibiotic

TET = Tetracycline

WHO = World Health Organization

ACKNOWLEDGMENTS

I would like to thank my supervisors Päivi Tammela, Heidi Kidron and Cristina Durante Cruz for sharing their knowledge, expertise, guidance and mental support during the experimental and written parts of my master thesis. With no prior experience in lab work, I felt slightly nervous in last March when I was about to start my master thesis project. I am greatly thankful for Cristina who perfectly took into account my non-existent research background, teaching me the basics of microbiological methods and encouraging me to take an active role in the literature search, execution and design of assays and data analysis from the very beginning of the project. I would like to thank Päivi, Heidi and Cristina for being easily reachable both face-to-face and by email whenever I needed assistance in terms of analyzing or interpreting the results and making decisions regarding the strain, efflux pump inhibitor or antibiotic selection. Weekly discussions with Cristina and frequently arranged meetings with all supervisors assured that the progress was regularly assessed, and the objectives of the project were eventually met. Even though this was my own project, thanks for the well-organized and structured supervision, I did not feel like left alone. I feel humble and honored that Päivi and Heidi had trust on me and let their project to be my project during these five months in the lab.

I would also like to thank Polina Ilina for kindly sharing her knowledge in automated liquid handling and helping with programming and optimizing the Biomek i7 protocol, thus enabling the use of Biomek i7 Automated Workstation in the checkerboard assays. I would also like to thank the rest of Bioactivity Screening Group for taking me as a part of the group and creating such a warm and welcoming atmosphere both in the office and in the lab. Prior to the master thesis project, I had no idea what research truly is but after seeing a glimpse of it, I really enjoyed at creating something with a true value and meaning.

1 INTRODUCTION

Global Antimicrobial Resistance Surveillance System (GLASS) was founded by World Health Organization (WHO) in 2015 (WHO, 2017a). The aims of this launch were to improve the understanding of the real extent of antimicrobial resistance (AMR) worldwide and standardize the collection of AMR surveillance data within member countries, thus providing a framework for AMR surveillance system. The first report released in January 2018 summarizes the data collected in 22 countries in 2016 regarding the level of AMR for selected bacteria. Unfortunately, these findings were in line with the global report of AMR published by WHO in April 2014, showing that AMR is widely spread, it does not acknowledge national borders and it is alarmingly high in some countries (WHO, 2014). For instance, resistance to ciprofloxacin in urinary tract infections caused by *Escherichia coli* varied within the range 8% to 65%, which is problematic as ciprofloxacin is commonly used in the treatment of this condition (WHO, 2017a). Carbapenem-resistant *Acinetobacter baumannii*, prioritized by WHO in terms of allocating resources in the research and development of novel antibiotics (ATBs) against it, has reached resistance rate as high as 75% in Asia (WHO, 2017a; 2017b). This finding needs to be taken seriously as there is a high rate of resistance to nearly all ATBs existing for the treatment of *A. baumannii*-related infections. In fact, without any new effective ATBs or novel approaches to restore the efficacy of existing ATBs, the post-antibiotic era where common community-acquired infections are fatal again, could hypothetically become true (WHO, 2014).

AMR is accelerated by the overuse and misuse of ATBs both in humans and in animals: in the presence of noxious agents, for instance sub-inhibitory concentrations of ATBs (that do not inhibit bacterial growth), bacteria attempt to survive in their environment by increasing the extrusion of noxious compounds via efflux pumps (EPs) (Viveiros *et al.*, 2005). The number of EPs expressed by Gram-negative bacteria (GNB) is limited and in normal conditions many EP systems are even poorly expressed (Nishino *et al.*, 2009). If the concentration of noxious compounds exceeds the extrusion capacity of EPs, the gene expression may be up-regulated as a consequence. This is mostly mediated by mutations in the regulatory network of EP genes, leading to overexpression of EP systems. In fact,

an analysis by quantitative real-time reverse transcriptase-polymerase chain reaction (RT-qPCR) methodology revealed that the gene expression of EPs was up-regulated after the inducement of tetracycline-resistance in parental and efflux-deficient *E. coli* K-12 strains (Viveiros *et al.*, 2005). Interestingly, resistance of tetracycline-induced, efflux-deficient *E. coli* K-12 to ATBs was similar to that of tetracycline-induced, isogenic parental strain even though one of the EP systems was deleted within this mutant strain. This finding verified that the regulation of EP gene expression is cross-linked (the function of deleted EP will be compensated by the overexpression of other EPs) and demonstrated that the overuse and misuse of ATBs converts this intrinsic resistance mechanism of GNB into acquired multidrug resistance (MDR).

Pharmaceutical industry has lost its interest in developing new antibacterial agents because ATBs are not as profitable as drugs used in the treatment of chronic diseases, such as diabetes, coronary-heart and autoimmune diseases (Ventola, 2015). ATBs are used for a relatively short period of time and the costs of one ATB course are low. Furthermore, novel ATBs are usually considered as the last-resort treatment and saved for serious infections with no susceptibility to any other ATBs. For these reasons, pharmaceutical companies are afraid of not having return to their enormous financial investments during the drug development. However, research to find solutions to address AMR is undoubtedly paramount and cannot be dismissed. In fact, AMR causes the extension of treatment and hospitalization, disability and in the worst case leads to death. Additionally, it forces to the use of last-resort ATBs which are more expensive, eventually resulting in high costs at individual and societal level, or even out of reach at some settings (i.e. developing countries).

This thesis will focus on GNB *E. coli*, which is on the WHO priority pathogens list in terms of investing resources on the drug research and development (WHO, 2017b). *E. coli* is a part of the microbiota in the mammalian gut and the main cause for both community and hospital-acquired urinary tract and bloodstream infections (WHO, 2017a).

2 LITERATURE REVIEW

2.1. Obstacles in the development of novel antibacterial compounds against GNB

The discovery and design of novel antibacterial compounds against GNB-related infections is challenging because of a dual defense mechanism encompassed by GNB (Tommasi *et al.,* 2018). The outermost layer of bacterial cell envelope will be discussed first as this permeability barrier is a characteristic feature for GNB and it highly contributes to the challenges in developing novel antibacterial agents that are capable of permeating the outer membrane (OM) and reaching the periplasmic and cytosolic drug targets. In addition to retarded cellular uptake, the intracellular concentration of antibacterial agent may not attain the level required for the bacteriostatic or bactericidal activity of ATB if it is actively pumped out of the bacterial cell to the external medium. Indeed, in this thesis the focus will be on the efflux activity that is altered under prolonged exposure to ATBs at their sub-inhibitory concentrations and thus plays a crucial role in the ever-increasing emergence of bacterial MDR. Furthermore, the strategies to reduce the bacterial efflux activity are introduced, focusing on efflux pump inhibitors (EPIs) as a promising co-therapy approach to overcome this global public health threat.

2.1.1. The structure of bacterial cell envelope sets challenges on the drug permeability

E. coli belongs to the microbiota in the mammalian gut and for survival in the presence of high concentration of cell membrane-disrupting bile salts, retarded influx and enhanced efflux rates of chemicals are needed (Thanassi *et al.*, 1997; Silhavy *et al.*, 2010). There are three key features in the cell wall structure which are found in all GNB: the OM, the cell or inner membrane (IM) as the innermost layer and the periplasm as an aqueous cellular compartment which is delimited by these two bilayers (Figure 1A). A thin peptidoglycan layer within the periplasmic space defines the bacterial cell shape and it consists of alternating monosaccharide units of N-acetylglucosamine and N-acetylmuramic acid, building up to long polymeric strands which are further cross-linked to each other by oligopeptide side chains. Because bacterial cells lack intracellular organelles, all essential cell functions, like energy metabolism, take place on the IM.

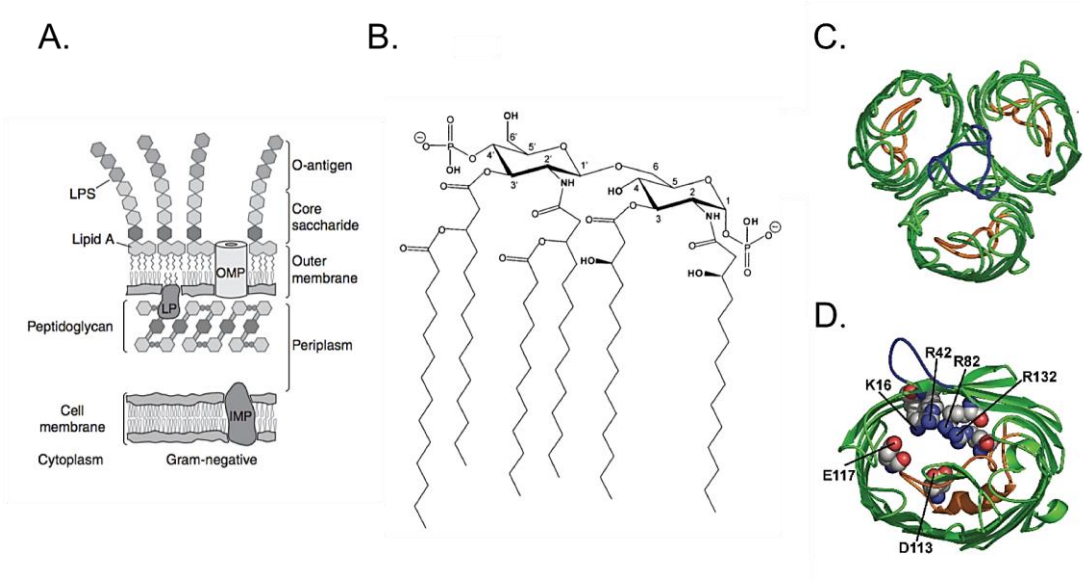

Figure 1. A. The cell wall structure of Gram-negative bacteria consists of outer membrane, inner membrane and the periplasmic space delimited by these two bilayers. **B.** The backbone of lipid A is comprised of two glucosamines and is phosphorylated at positions 1 and 4 and acetylated with four saturated, hydroxy fatty acids at positions 2, 2', 3 and 3'. **C.** OmpF is a trimeric porin and the outer membrane protein of *E. coli* and each of these monomeric units have adopted β-barrel conformation. **D.** The essential amino acid residues within the constriction area are shown: Glu117 and Asp113 from the loop 3 and Arg132, Arg82, Arg42 and Lys16 from the β-barrel wall of the constriction area are involved with establishing interactions between OmpF channel and translocating substrate (adapted from Nikaido, 2003; Silhavy *et al.*, 2010).

OM is an extra layer of protection and the first-line of defense from external noxious compounds in the hostile environment (Nikaido, 2003; Delcour, 2009). This permeability barrier needs to be overcome in order to access periplasmic and cytosolic drug targets. OM is an asymmetric bilayer which consists of phospholipids in the inner leaflet and lipopolysaccharides (LPS) in the outer leaflet. LPS themselves are comprised of three parts: lipid A, the core oligosaccharide with 6 to 10 monosaccharide units and O-antigen, which triggers the host immune system, as the outermost part of the structure (Figures 1A–B). Anionic phosphate groups in the glucosamine backbone of lipid A and several negatively charged residues in the oligosaccharide core strongly bind divalent cations, resulting in a tightly-packed structure as the electrostatic repulsion generated between neighboring LPS molecules is compensated by divalent cations. Furthermore, there are exceptionally many hydrogen bond donors in the glucosamine backbone of lipid A and

in hydroxy fatty acids acylated at positions 2, 2', 3 and 3' as seen in Figure 1B. Hydrogen bonds formed between neighboring LPS molecules further stabilize the structure and make the permeation through the OM even more challenging for hydrophobic antibacterial agents. Additionally, the low fluidity of lipid moiety of LPS molecules makes the OM even less permeable for these compounds. Each LPS molecule have six to seven saturated fatty acids instead of two and this fundamental difference between LPS molecules and phospholipids increases the rigidity of OM structure (Figure 1B).

Two distinguishable pathways to the interior of bacterial cells have been acknowledged: lipid-mediated and porin-mediated pathways (Delcour, 2009). Hydrophobic antibacterial agents including aminoglycosides, macrolides, rifamycins and cationic peptides reach the interior of bacterial cells by permeating through the lipid bilayer of the OM. Hydrophilic molecules utilize membrane-spanning protein structures called porins for translocation over the OM. Porins can be classified according to their substrate specificity and functional structure (Pagès *et al.*, 2008). Inside these water-filled channels, there is a constriction area comprised of negatively and positively charged residues (Figure 1D) (Nikaido, 2003; Pagès *et al.*, 2008). This constriction area is involved with the translocation of small (less than 700 Da) hydrophilic antibacterial compounds, for example β-lactams, quinolones and tetracyclines, through the channel via intermolecular interactions generated between the substrate and the amino acid side chains. Single amino acid substitutions within this constriction area resulted in impaired ATB diffusion by hindering the translocation of antibacterial agents through the channel and thus indicating the importance of these residues in the substrate translocation (Simonet *et al.*, 2000).

The importance of the OM in the intrinsic MDR has been acknowledged in the studies with influx-deficient *E. coli* strain, lacking non-specific OmpF porins, where it was shown that the MIC value (known as the lowest concentration of ATB that prevents visible bacterial growth) of quinolones increased compared to that of wild-type *E. coli* strain (Hirai *et al.*, 1986; CLSI, 2015). However, the retarded ATB influx due to this permeability barrier is not the only contributor to the intrinsic MDR. In fact, EPs either driven by ATP hydrolysis or proton motive force (PMF), may function at a high efficiency, eventually resulting in the imbalance between influx and efflux rates. In many

cases, the intrinsic MDR is the sum of these two phenomena: low influx and high efflux rates (Li and Nikaido, 2004). In the following chapters, the contribution of EPs to both intrinsic and acquired MDR are profoundly discussed starting with the depiction of EP structure and function and thereafter introducing the strategies to reduce the enhanced efflux activity.

2.1.2. EPs play an essential role in acquired MDR but have some physiological functions as well

To date, there are five different EP superfamilies associated with MDR: ATP-binding cassette (ABC) driven by ATP hydrolysis, resistance nodulation division (RND), major facilitator (MFS), multidrug and toxic compound extrusion (MATE) and small multidrug resistance (SMR) -superfamilies, all of them driven by the PMF (Li and Nikaido, 2004; Mahamoud *et al.*, 2007). The focus of this thesis will be on the AcrAB-TolC EP system, a tripartite protein complex with a fully characterized crystal structure, which belongs to the RND-superfamily and is the most abundant MDR EP system in *E. coli* (Li and Nikaido, 2004; Anes *et al.*, 2015). Transporters belonging to other superfamilies are also found in *E. coli*, for instance MacAB in the ABC-superfamily, EmrAB in the MFS-superfamily and EmrE in the SMR-superfamily, but AcrAB-TolC is the most extensively studied EP system and it predominantly contributes to both intrinsic and acquired MDR in *E. coli* (Sulavik *et al.*, 2001).

RND-type EPs can be divided into two subgroups depending on if they are involved with exporting amphiphilic and hydrophilic compounds or heavy metals (Anes *et al.*, 2015). Within the hydrophilic and amphiphilic efflux RND (HAE-RND) -family there are five different transporters, AcrAB, AcrAD, AcrEF, MdtABC and MdtEF. Within the heavy metal efflux RND (HME-RND) -family there is only one transporter, CusCFBA. All of these transporters are connected to the OM by the TolC channel, which means that *tolC* gene deletion prevents all six EPs within the HAE-RND and HME-RND -families from assembling. In previous studies both TolC- and AcrAB-deleted *E. coli* strains have been used as a control strain (Matsumoto *et al.*, 2011; Opperman *et al.*, 2014). If an antibacterial agent is not selectively pumped out via the AcrAB transporter but several transporters within the HAE-RND -family contribute to the total extrusion of the

antibacterial agent instead, the MIC value obtained for TolC-deleted *E. coli* strain is presumably lower than that of AcrAB-deleted *E. coli* strain, also demonstrated in the study by Sulavik *et al.* (2001). In the same study, it was noted that the susceptibility to ATBs was higher in an *E. coli* strain with multiple deleted transporters within the HAE-RND -family than in AcrAB-deleted *E. coli* strain, indicating that other EP systems within the RND-superfamily also contribute to MDR.

However, EP systems are not only associated with ever-increasing emergence of MDR: it seems that these same pumps are important for the bacterial survival in the hostile environments (Thanassi *et al.*, 1997). In other words, EPs are expressed at certain basal level in normal conditions to export external noxious compounds and thus defend bacteria from toxic effects of these compounds. Additionally, there is accumulated evidence of MDR EP systems playing a role in the bacterial pathogenesis and virulence by excreting virulent determinants and evading host-defense mechanisms and host-derived antibacterial substances (Hirakata *et al.*, 2002; Piddock, 2006; Hirakata *et al.*, 2009; Padilla *et al.*, 2010; Pérez *et al.*, 2012). Therefore, EPs are an extremely interesting drug target because not only the resistance to existing antibacterial agents could be reversed but also the ability of bacteria to colonize host cells and cause infections could be counteracted by targeting to these EP systems.

2.2. AcrAB-TolC – a tripartite protein complex extruding a broad repertoire of structurally unrelated compounds

2.2.1. The structure of AcrAB-TolC

AcrAB-TolC is a tripartite protein complex which consists of an OM channel TolC, an IM transporter AcrB and a membrane-fusion protein AcrA which works as a linker between the TolC channel and the AcrB transporter (Figure 2A) (Murakami *et al.*, 2006; 2008). TolC is a trimeric protein structure partially residing in the OM and partially protruding to the periplasmic compartment (Koronakis *et al.*, 2000; Eswaran *et al.*, 2004). The transmembrane domain of TolC channel is comprised of twelve antiparallel and right-twisted β-strands, each monomer contributing to four strands (Figure 2B). This

domain adopts the β-barrel conformation with a large, solvent-filled central cavity which is the uppermost part of the continuous, sealed conduit traversing from the central funnel of the AcrB transporter through the periplasmic domain of the TolC channel (Du *et al.*, 2014). The periplasmic domain of TolC consists of twelve antiparallel and left-twisted α-helices and each monomeric subunit has two long α-helices, extending from the junction of β-strands and α-helices to the very proximal end of TolC, and two pairs of short α-helices stacked one upon another (Figure 2B). The periplasmic domain also adopts the barrel conformation. Six pairs of coiled coils seal the proximal end of the α-helical barrel, each monomer contributing to two pairs.

AcrB is a homotrimeric IM transporter which is responsible for both substrate specificity and energy production (Murakami *et al.*, 2006; 2008; Seeger *et al.*, 2006; Du *et al.*, 2014). Each monomeric subunit, protomer, is comprised of twelve transmembrane α-helices and divided into three domains: the uppermost is the TolC-docking domain, the middle one is the porter domain and the innermost is the transmembrane domain (Figure 2A). The deep distal binding pocket (DBP) exists in the AcrB porter domain and it is rich in phenylalanine residues (Figure 2C). The crystal structures of the AcrB porter domain with minocycline and doxorubicin have shown that binding via hydrophobic interactions takes place at this phenylalanine cluster region. In addition, there are some polar residues within this region and hydrogen bonds may partly contribute to these intermolecular interactions. However, the set of residues used for binding varies and the exact binding sites of minocycline and doxorubicin are not identical. Furthermore, the crystal structures of rifampicin- and erythromycin-bound AcrAB transporter have shown that high-molecular mass antibiotics (HMMAs) are not accommodated at the same phenylalanine rich region as small-molecular mass antibiotics (SMMAs) (Nakashima *et al.*, 2011; Cha *et al.*, 2014). In fact, another binding pocket separated from the DBP by the switch-loop was identified. The capacity of AcrAB-TolC tripartite protein complex to extrude a broad range of structurally unrelated compounds can be explained by the existence of two binding pockets in the AcrB porter domain. In addition, substrates can adopt different alignments and conformations within the same binding pocket depending on the set of residues used for binding.

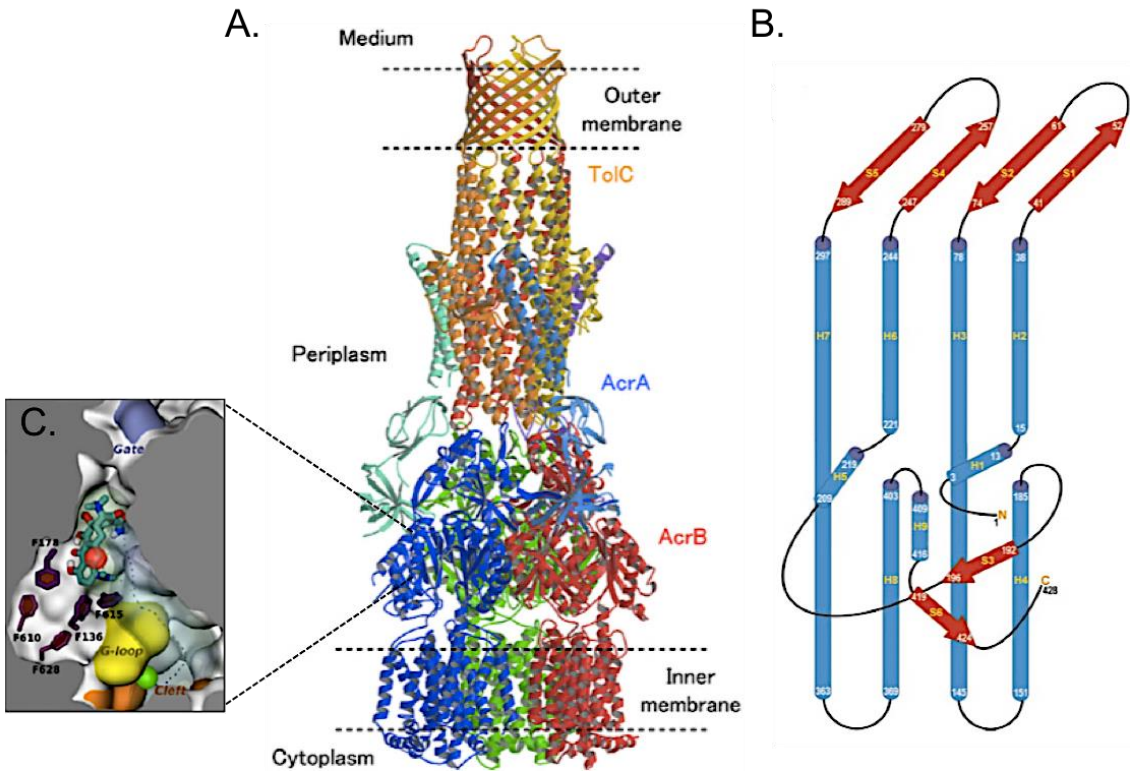

Figure 2. A. The crystal structure of AcrAB-TolC tripartite protein complex (adapted from Murakami *et al.*, 2008). **B.** A subunit of TolC consists of four antiparallel, right-twisted β-strands located in the outer membrane (red) and four antiparallel, left-twisted α-helices located in the periplasm (blue) (adapted from Koronakis *et al.*, 2000). **C.** The substrate of the AcrB porter domain, minocycline, and phenylalanine residues in the deep distal binding pocket are illustrated as stick drawings (adapted from Opperman and Nguyen, 2015).

An AcrA hexamer mediates the cooperation of the AcrB transporter and the TolC channel (Eswaran *et al.*, 2004; Du *et al.*, 2014). This periplasmic adaptor protein stabilizes the assembly of the tripartite protein complex, mediates the conformational change from the AcrB transporter to the TolC channel and thus triggers the entrance opening at the proximal end of α-helical barrel. In addition, this accessory protein may have an effect on the substrate specificity of AcrB (Krishnamoorthy *et al.*, 2008).

2.2.2. The function of AcrAB-TolC

Due to a small internal diameter of the central pore of AcrB (16 Å), the hypothesis that EP substrates are translocated straight from the central pore to the central funnel of the TolC-docking domain and further to the TolC channel was rejected (Eicher *et al.*, 2009; Du *et al.*, 2014). Instead, Murakami *et al.* (2006; 2008) proposed a three-step functionally rotating mechanism where the conformational states of loose (L), tight (T) and open (O) consecutively rotate and in each functional state of the export cycle protomers adopt different conformation (Figure 3A). The access protomer is in the L state, the binding protomer in the T state and the extrusion protomer in the O state, respectively.

In the L state, the periplasmic cleft above the membrane plane is accessible for EP substrates in the periplasm (Figure 3B) (Eicher *et al.*, 2009; 2012; Anes *et al.*, 2015). In addition, there is another vestibule which captures EP substrates from the outer leaflet of the IM and the cytosol. The binding at the DBP in the AcrB porter domain occurs after some conformational changes in the switch-loop (which separates two binding pockets from each other) and in the helices which delineate the DBP, thus making it wide enough to accommodate a broad range of structurally unrelated compounds. HMMAs, for instance macrolides, are also accommodated by the DBP along their translocation pathway because the internal diameter of the DBP in the T state is larger than that in the L state (Cha *et al.*, 2014). However, the actual binding of HMMAs occurs at the proximal binding pocket (PBP) during the L state of the export cycle. Thereafter, HMMAs are forced to the DBP by a peristaltic mechanism and they are eventually extruded to the central funnel of the TolC-docking domain (Nakashima *et al.*, 2011). In contrast, SMMAs are bound to the DBP of the binding protomer in the T state. Interestingly, it was shown that doxorubicin and rifampicin can be simultaneously bound, rifampicin at the PBP of the access protomer in the L state and doxorubicin at the DBP of the binding protomer in the T state. It was further demonstrated that replacing one residue of the switch-loop with another amino acid reverses the resistance to HMMAs (Cha *et al.*, 2014). It was noted that the switch-loop of this AcrB-variant in the L state was conformationally similar to that of AcrB-wild type in the T state, meaning that the binding of macrolides at the PBP was sterically hindered by the switch-loop (Eicher *et al.*, 2012).

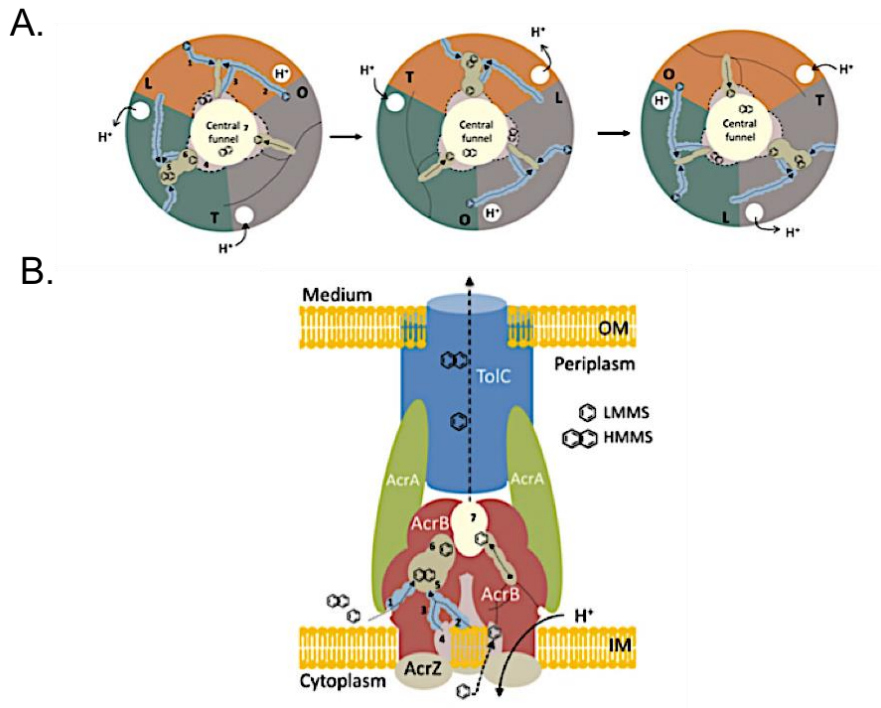

Figure 3. A. Top view of AcrB porter domain and **B.** side view of AcrAB-TolC tripartite protein complex illustrating the translocation of efflux pump substrates in the consecutive conformational states, loose (L), tight (T) and open (O). In the side view, the left protomer of AcrB porter domain is in the L state when it is binding high-molecular mass substrate (HMMS) at the proximal binding pocket (5) and in the T state when it is binding low-molecular mass substrate (LMMS) at the deep distal biding pocket (6), respectively. The right promoter of AcrB porter domain is in the O state, extruding the substrate to the central funnel of the TolC-docking domain (7) and further to the TolC channel (adapted from Anes *et al.*, 2015).

The transition from the T to the O conformational state is thought to be the energy-requiring step in the three-step functionally rotating mechanism and during this transition the exit pathway towards the central funnel of the TolC-docking domain is opened as the α-helix of extrusion protomer is tilted away (Figure 3B) (Murakami *et al.*, 2006; 2008; Seeger *et al.*, 2006; Eicher *et al.*, 2009; 2012). The intramolecular tunnels are collapsed resulting in the unidirectional translocation of EP substrates towards the TolC channel and eventually to the external medium outside the bacterial cells. It was proposed that the proton translocation site is located in the AcrB transmembrane domain and protonation results in the re-orientation of Lys940 residue (Seeger *et al.*, 2006; Murakami *et al.*, 2008; Eicher *et al.*, 2009). In the L and the T conformational states, the Lys940 residue is surrounded by Asp407 and Asp408 residues and forms ion bonds with carboxyl acid groups of these two aspartates. However, the shift from the T to the O state makes these

residues orientate differently: the uptake of proton at the translocation site dissociates ion bonds between Lys940 and Asp407/408 and triggers the re-orientation of Lys940 towards Thr978. The reversion to the L state requires the release of proton. However, it is still not completely understood how these subtle conformational changes in the AcrB transmembrane domain are linked to the conformational changes in the AcrB porter domain and further observed as the entrance opening at the periplasmic end of TolC channel. Thus, for fully understanding the cooperation of AcrB transporter, AcrA adaptor protein and TolC channel, more studies are required.

2.2.3. The inhibition of efflux activity – a promising approach to combat MDR in GNB

It is necessary to be familiar with the structure and the function of MDR EP systems in order to understand how an increased efflux activity could be inhibited. The first co-crystal structure of AcrAB transporter and EPI was published in 2013 by Nakashima *et al.* and thereafter molecular dynamics (MD) simulations has been used as a tool of choice for characterizing the essential residues for establishing AcrAB–EPI complexes (Vargui *et al.*, 2014). However, it is still a long way to go until *de novo* drug design methods could be utilized in the development of improved bacterial EPIs as the knowledge of substrate–EP interactions is not fully comprehensive as yet. In principle, all three components of AcrAB-TolC EP systems could be targeted to inhibit an enhanced efflux activity (Figure 4) (Pagès and Amaral, 2009; Venter *et al.*, 2015). Koronakis *et al.* (2000) demonstrated that the electronegativity of the interior surface of the TolC channel cavity increases when moving towards the proximal end of α-helical barrel. Thus, the export of EP substrates via the TolC channel could be inhibited by blocking this entrance using large cationic molecules. Alternatively, the binding of EP substrates within the AcrB porter domain could be hindered either by competing with the same binding site or acting as a steric blocker (Pagès and Amaral, 2009; Venter *et al.*, 2015). Also, “locking” the switch-loop in the L state conformation could prevent the translocation of EP substrates between two binding pockets.

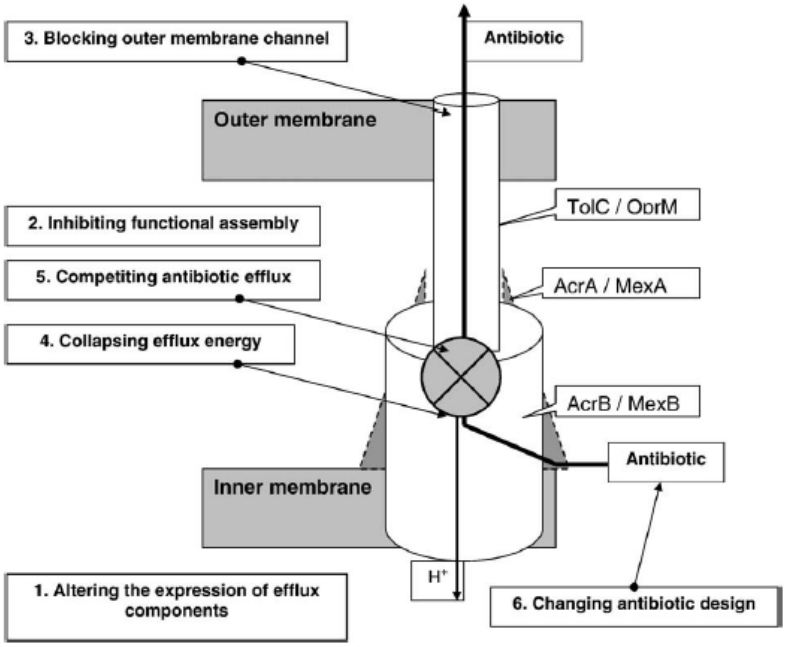

Figure 4. Possible mechanisms to reduce efflux activity (Pagès and Amaral, 2009).

By activating local and global gene repressors, AcrR and MarR, and inhibiting global gene activators, SoxS, Rob and MarA, the gene expression of EPs could be down-regulated (Nishino *et al*., 2009; Venter *et al.*, 2015). As RND-type EPs are energized by the PMF, the pump function could also be abolished by collapsing the proton gradient and the electric potential across the bacterial cell envelope (Pagès and Amaral, 2009). Uncoupling of oxidation-phosphorylation reaction will result in the depletion of ATP production as the protons generated during the electron transport chain and pumped out of the bacterial cell to the outer leaflet of the OM will not be taken back into the cell through ATP synthases (Terada, 1990). In contrast, an ionophore transports protons from the external medium to the interior of the bacterial cell, dissociates and leaves the cell in the anionic state, eventually dissipating both the proton gradient and the electric potential. As the uncoupling action is not specific to bacterial cells, the major drawback associated with the use of ionophores is the cytotoxicity towards mammalian cells.

2.3. EPIs

Ideally, novel EPIs that have shown to restore the susceptibility of efflux-overexpressing *E. coli* strain to antibacterial agents would be effective towards other MDR GNB, meaning that the same EPI could be used in the treatment of other MDR GNB-related infections. However, this means that EP systems expressed by different GNB should show similarity in their primary and tertiary protein structures. Opperman *et al.* (2014) studied the spectrum of activity of a novel EPI (MBX2319) towards other GNB bacteria than *E. coli*: at least 4-fold decrease in the intrinsic MIC values of fluoroquinolones was achieved in *Shigella flexneri*, *Salmonella enterica* and *Enterobacter aerogenes*, meaning that it could be possible to have an EPI with potency not only towards *E. coli* but also against other GNB. In contrast to what could have been expected based on the structural similarity between AcrAB in *E. coli* and MexAB in *P. aeruginosa*, only limited activity against *P. aeruginosa* was observed. However, the authors speculated that by modifying the molecular structure of EPI, the spectrum of activity could be extended to *P. aeruginosa* as well.

The term EPI is controversial. It has been criticized to be misleading because the compounds classified as EPIs in the literature do not mediate their efflux inhibitory activity directly by competing with the same binding site as substrates (Amaral *et al.*, 2014). In fact, it was proposed that efflux pump modulators should be primarily used when discussing this topic. Even though this incorrect use of terminology is acknowledged here, compounds with efflux inhibitory activity will be referred as EPIs here in the thesis for clarity and concordance with the published studies.

2.3.1. Carbonyl cyanide 3-chlorophenylhydrazone (CCCP)

CCCP is a protonophore and an uncoupler of oxidation-phosphorylation reaction (Kadenbach, 2003). The cytotoxicity of CCCP is explained by the uncoupling of oxidation-phosphorylation reaction as the ATP production and energy-requiring cellular functions will be interfered (Naseem *et al.*, 2009; Sekyere and Amoako, 2017). In fact, the energy generated in the redox reactions of the electron transport chain cannot be used in the ATP synthesis. The mechanism of the uncoupling action is the transport of protons straight through the bacterial cell envelope instead of the uptake via ATP synthases (Terada, 1990). As a weak acid, CCCP crosses the bacterial cell envelope (that is impermeable for protons as such) in the protonated state and releases the proton in the intracellular compartment. Because of the aromatic and conjugated structure of CCCP, the negative charge is delocalized across the entire molecule and thus the electric field surrounding CCCP is weaker than it would be if the negative charge was localized on one atom (Kadenbach, 2003). This phenomenon enables free diffusion of CCCP in the anionic state across the bacterial cell wall back to the extracellular medium. As a result, both pH gradient and electric potential are dissipated. The PMF consists of pH gradient and electric potential and whether one of them (or both) is interfered, the PMF will be degraded and AcrAB-TolC EP system will not have the source of energy required for the shift from the T to the O conformational state in the three-step functionally rotating mechanism (Terada, 1990; Seeger *et al.*, 2006; Farha *et al.*, 2013). Because several MDR-superfamilies, such as the RND, the MFS and the SMR, are powered by the PMF, selectivity towards one specific EP system of interest will not be achieved using CCCP (Mahamoud *et al.*, 2007).

2.3.2. Phenylalanine-arginyl β-naphthylamide (PAβN)

PAβN is a peptidomimetic that works not only as an EPI of AcrAB and AcrEF transporters of *E. coli* but also as an OM permeabilizer at higher concentrations in efflux-proficient strains but at lower concentrations in efflux-deficient strains (Misra *et al.*, 2015). Based on the MD simulations, a dual mechanism for efflux inhibitory activity of PAβN was suggested (Vargiu *et al.*, 2014). Firstly, PAβN prevents the movement of the switch-loop that plays an important role in the substrate translocation between PBP and

DBP during the transition between the L and T conformational states of the three-step functionally rotating mechanism. Secondly, PAβN occludes the translocation pathway and reduces the space available for substrates, thus hindering the binding of substrates at the upper part of DBP.

PAβN is a positively charged dipeptide analog that increases the OM permeability by interfering with divalent cations responsible for cross-linking the adjacent LPS molecules (Sawyer *et al.*, 1988; Piers and Hancock, 1994; Mojsoska and Jenssen, 2015). Matsumoto *et al.* (2011) observed that the intrinsic MIC value of ciprofloxacin, which readily enters into the bacterial cell, did not change in the presence of PAβN but for erythromycin, whose entry into the bacterial cell is more restrained, a 16-fold decrease in the intrinsic MIC value was recorded. The intrinsic MIC value of antibacterial agents in efflux-deficient *E. coli* strain should not change regardless of the introduction of EPI (Lomovskaya *et al.*, 2001). However, the intrinsic MIC value of low-permeability HMMAs may decrease in the presence of an EPI with an OM permeabilizing activity (Matsumoto *et al.*, 2011). Another study supporting the OM permeabilizing effect of PAβN was carried out by Bohnert and Kern (2005). In this study the intrinsic MIC value of rifampicin, a poor substrate of the AcrAB-TolC EP system, was decreased by 128-fold in efflux-deficient *E. coli* strain after the addition of PAβN.

Misra *et al.* (2015) concluded that the secondary effect of PAβN, which is the increased OM permeability, is greatly amplified in efflux-deficient bacterial cells. This finding is explained by an impaired removal of PAβN, which is a substrate of RND-type EPs, out of the bacterial cells and thus even lower concentrations of PAβN are sufficient to cause disruption in the OM. In fact, Matsumoto *et al.* (2011) observed that in a TolC-deleted *E. coli* strain the fluorescence intensity of intracellularly accumulated fluorescein started to disappear when PAβN was tested at the concentration of 4 μg/ml, indicating that fluorescein, which is a fluorescent end-product of fluorescein-di-β-d-galactopyranoside (FDG) hydrolysis by cytoplasmic β-galactosidase and a substrate of RND-type EPs, was leaked out to the external medium as the result of increased OM permeability. In contrast, the primary effect of PAβN in efflux-proficient bacterial cells is the inhibition of AcrAB and AcrEF transporters when PAβN was tested up to the concentration of 20 μg/ml and

the secondary effect of PAβN was postulated to be seen only at higher concentrations (Misra *et al.*, 2015). However, an exact threshold value between low and high concentrations was not defined by these authors.

2.3.3. 1-(1-Naphthylmethyl)-piperazine (NMP)

NMP is an arylpiperazine that has been shown to increase the intracellular accumulation of ethidium bromide, a substrate of AcrAB-TolC and AcrEF-TolC EP systems, in AcrAB- and AcrEF-overexpressing but not in efflux-deficient *E. coli* strains, suggesting its role as an inhibitor of AcrAB and AcrEF transporters (Bohnert and Kern, 2005). Kern *et al.* (2006) proposed that different spectrum of antibacterial agents potentiated by PAβN and NMP could be explained by the different modes of action and dissimilar binding sites of the EPIs within the DBP, meaning that only the substrates bound to exactly the same site as the EPI are not expelled out of the bacterial cells. However, based on the MD simulations carried out by Vargiu *et al.* (2014) seven out of twelve residues contributing to the binding of EPI were the same for PAβN and NMP, meaning that the binding sites of PAβN and NMP were not as dissimilar as suggested by Kern *et al.* (2006).

In MD simulations, NMP was only partly located in the hydrophobic trap at the lower part of the DBP – instead, the residues of the switch-loop greatly contributed to the intermolecular interactions between NMP and AcrAB transporter (Vargiu *et al.*, 2014). The same inhibition mechanism as for PAβN was proposed: the closure of the upper part of the DBP prevents the EP substrates, such as minocycline, from binding at this site and "locking" the switch-loop in the L state conformation inhibits the translocation of substrates between two binding pockets. To date, there are no studies or evidence of the OM permeabilizing effects of NMP (Opperman and Nguyen, 2015). However, NMP is not an ideal EPI either and it has not proceeded to the advanced clinical trials due to its serotonin agonist properties (Bohnert and Kern, 2005).

By a random mutagenesis approach focused on the AcrB porter domain, Schuster *et al.* (2014) managed to generate a NMP-resistant *E. coli* strain with two mutations in the residues located within the binding protomer of the AcrB porter domain. The objective

of this study was to identify the residues essential for the establishment of NMP–AcrAB complexes and by substituting these residues with another amino acids, NMP could not exert its therapeutic action as the potentiator of the antibacterial efficacy of ATBs. However, the binding site of NMP mapped by MD simulations (Vargiu *et al.*, 2014) did not include these two residues which were concluded by Schuster *et al.* (2014). to be important in terms of establishing NMP–AcrAB complex. Later it was hypothesized that these residues mapped by a random mutagenesis approach may play an important role in NMP-induced conformational changes and by substituting these residues with another amino acids, NMP cannot induce conformational changes in the upper part of DBP and thus hinder the binding of antibacterial agents within DBP.

2.3.4. Mefloquine

Mefloquine is a quinolone derivative that is the first-line anti-malarial drug in the areas of chloroquine-resistant *Plasmodium falciparum* and it is suitable to be used for malaria chemoprophylaxis in long-term travelers, pregnant and breastfeeding women and small children (Schlagenhauf *et al.*, 2010). Studies have suggested that mefloquine inhibits the oxidation of NADH and therefore interferes with the bacterial respiratory chain and energy metabolism (Brown *et al.*, 1979). Mefloquine was also shown to damage the bacterial cell wall leading to the release of DNA into the external medium (Kunin and Ellis, 2000). In addition, the antibacterial activity of gentamicin, a poorly permeable antibacterial agent, was improved in the presence of mefloquine derivative. To date, the efflux inhibitory activity of mefloquine has not been excessively studied and there is only a small number of studies where mefloquine was employed as an EPI in the checkerboard assays. Vidal-Aroca *et al.* (2009) demonstrated that mefloquine is a strong EPI for RND-type EPs but the exact mode of action was not discussed by these authors. The efflux inhibitory activity could partly be explained by the disruption in the OM integrity and energy metabolism, thus affecting the generation of protons pumped out of the bacterial cell and localized laterally on the OM (Brown *et al.*, 1979). For the future research perspectives, it would be interesting to define the exact mechanism behind the efflux inhibitory activity of mefloquine.

2.3.5. Thioridazine

Thioridazine is a phenothiazine that has been used as an antipsychotic drug for decades but the antibacterial activity of thioridazine, especially in killing intracellular MDR *M. tuberculosis*, has been acknowledged only recently (Amaral *et al.*, 2010). Thioridazine has also shown potential to be used as an adjuvant therapy with existing antibacterial agents that have lost potency towards GNB. Thioridazine indirectly inhibits efflux activity by blocking the binding of divalent calcium ions to the Ca^{2+}-dependent metabolic enzymes (Amaral *et al.*, 2010; Martins *et al.*, 2011). The dependency between intracellular Ca^{2+}-concentration and ATP production has been acknowledged, indicating that calcium is required for the activation of metabolic enzymes and therefore for the initiation of oxidation-phosphorylation reaction resulting in proton gradient across the bacterial cell envelope and ATP production (Naseem *et al.*, 2009). As previously described, the PMF is essential for the energy-requiring step of the three-step functionally rotating mechanism and for the pump function.

Chlorpromazine belongs to the same group of phenothiazines and the studies with chlorpromazine have confirmed the role of divalent calcium ions in normal pump function (Martins *et al.*, 2011). In fact, the efflux inhibitory activity of chlorpromazine could be abolished after the addition of calcium salt, meaning that the efflux inhibitory activity of phenothiazines is fully reversible. Thioridazine has shown to inhibit efflux activity especially at pH 8 because the maintenance of proton concentration on the outer leaflet of the OM and thus the maintenance of pump function is highly dependent on the metabolic energy at this pH (Amaral *et al.*, 2011). Protons dissociated from the cell surface to the bulk medium have to be replaced with the protons generated by energy metabolism. However, the proton replacement is not possible due to the inhibition of energy metabolism by thioridazine.

2.3.6. What is required for a good EPI?

Lomovskaya *et al.* (2001) introduced a list of criteria which novel compounds with efflux inhibitory activity should satisfy in order to be classified as true EPIs. The flowchart illustrated in Figure 5 has taken into account the criteria set for EPIs and the methodology used to confirm whether the assumptions are met. Firstly, if an EPI has some antibacterial activity, the intrinsic MIC value should be defined prior to the checkerboard assay and the EPI should be tested at the sub-inhibitory concentration (that is 4-fold lower than the intrinsic MIC of EPI itself, respectively) to minimize the chance that the synergism observed between EPI and antibacterial agent is caused by the antibacterial activity of the EPI itself (Bohnert and Kern, 2005; Coelho *et al.*, 2015). In the checkerboard assay, the EPI should not have any impact on the MIC value of antibacterial compounds that are not substrates of the EP system of interest (Lomovskaya *et al.*, 2001). Furthermore, an efflux-deficient strain has intrinsically lower MIC value than an efflux-proficient strain and the susceptibility to antibacterial agents should not be promoted by EPI in an efflux-deficient strain because the target of inhibition is deleted in this strain. On the other hand, the decrease in the intrinsic MIC value may reveal some unspecific modes of action, for instance the effect on the OM permeability (Misra *et al.*, 2015).

If the EPI potentiates the activity of ATBs in the checkerboard assay, it is important to find out whether this synergistic effect is mediated by the pump inhibition (Venter et *al.*, 2015). Efflux activity prior to and after the addition of EPI can be studied by following either the efflux or the accumulation of a fluorescent dye which is also a substrate of the EP system of interest. The accumulation of a fluorescent dye observed in an efflux-deficient strain is anticipated to be the maximum level of fluorescence obtainable and any increase in the steady-state level of fluorescence may be an indicative of enhanced dye influx rate, showing that the data generated in the accumulation assay could also be utilized to identify unspecific modes of action.

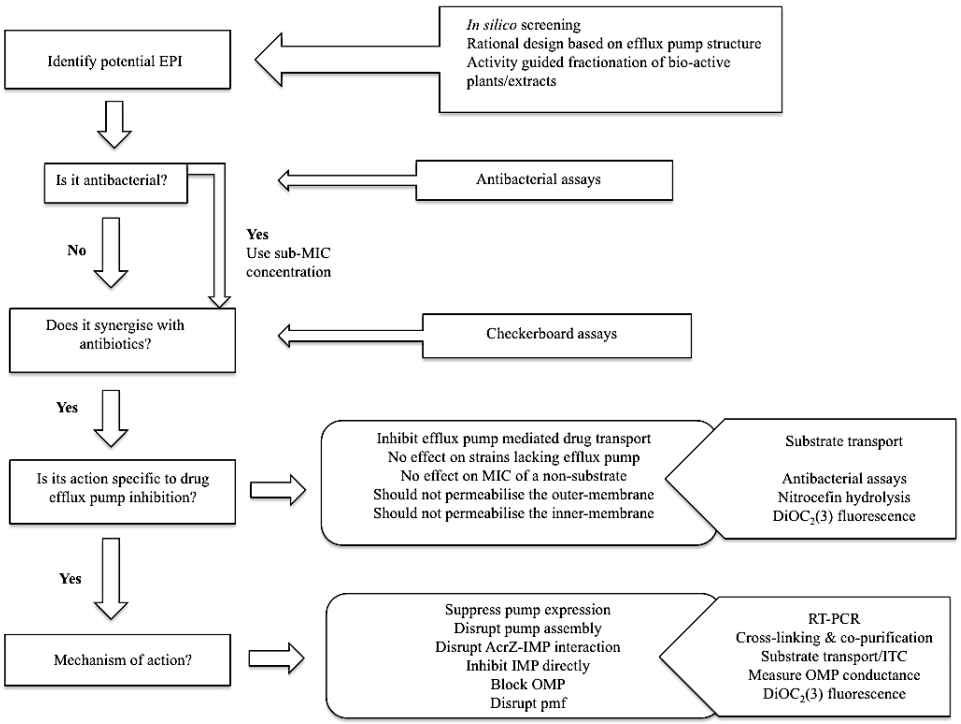

Figure 5. Flowchart for discovering new potential EPIs (adapted from Venter *et al.*, 2015).

As there are several different approaches to inhibit an increased efflux activity, the exact mode of action of EPI should be characterized: whether a novel compound with efflux inhibitory activity binds directly to the IM transporter (AcrB), blocks the OM channel (TolC), dissipates the PMF required for the energization of RND-type EPs, down-regulates the gene expression, suppresses the assembly of a tripartite protein complex or inhibits the interactions between the ancillary proteins (AcrA and AcrZ) and the IM and OM proteins. According to one of the criteria stated by Lomoskaya *et al.* (2001), a novel EPI should not interfere with the PMF because many mammalian cellular functions are also dependent on the proton gradient across the cell membrane and thus these compounds would be toxic against mammalian cells as well. Ideally, following the flowchart presented by Venter *et al.* (2015) the identification of positive hits in the high throughput screening (HTS) will eventually result in a true EPI with a desirable safety and efficacy profile. The need for novel EPIs is genuine as the commercially available EPIs have serious safety concerns mediated by the interference with the PMF and the OM permeability.

3 EXPERIMENTAL PART

3.1. Objectives

The purpose of this study was to identify the optimal assay conditions to be used in the future for HTS of novel EPIs. Stepwise progression of the experimental part is illustrated in the flowchart below (Figure 6). The project started with a larger number of *E. coli* strains (seven), EPIs (five) and ATBs (four) and step-by-step the number of the three factors were narrowed down. At the end, the optimal combination of one *E. coli* strain and one ATB was defined. Additionally, an EPI was selected to be used as a positive control in HTS to ensure the plate-to-plate reproducibility and reliability in the assay results and to work as a comparison for identified hits.

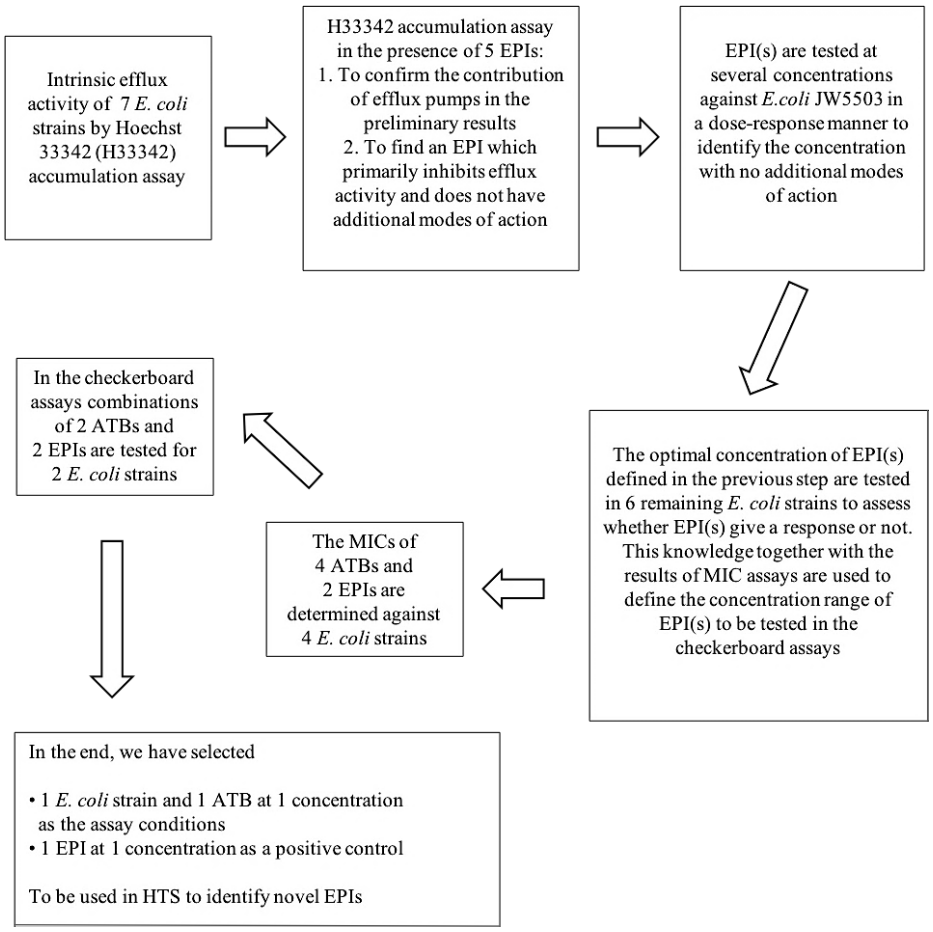

Figure 6. Schematic illustration of the steps required for achieving the final objective: the determination of the optimal assay conditions and a positive control to be used in high throughput screening.

3.2. Materials and methods

3.2.1. Bacterial strains

The project started with seven *E. coli* strains (see Table 1 for details), aiming to result in one *E. coli* strain with clinical relevance for the screening purposes. Based on the literature, *E. coli* JW5503, a TolC-deleted mutant strain, was a relevant control strain to assess whether new chemical entities (and compounds used here, already classified as EPIs in the literature) meet the criteria of being classified as true EPIs as stated by Lomovskaya *et al.* (2001). *E. coli* BW25113 is a parental strain for *E. coli* JW5503 and the inclusion of *E. coli* BW25113 in the study was important in order to enable the assessment of the contribution of efflux activity to the findings observed in Hoechst 33342 (H33342) accumulation assays and in the antibacterial susceptibility testing (Vidal-Aroca *et al.*, 2009). *E. coli* ATCC 25922 is a quality control strain that is widely used as a reference strain in the antibacterial susceptibility testing outlined by Clinical and Laboratory Standards Institute (CLSI) (2015). *E. coli* MG1655 is a strain used in many studies regarding EPIs and AMR (Matsumoto *et al.*, 2011; Iino *et al.*, 2012). Thus, these studies could be used as our reference for designing the assays. *E. coli* BAA1161 is an uropathogenic strain and the repertoire of wild-type pathogenic *E. coli* strains was complemented with two enteropathogenic strains, *E. coli* E2348 and *E. coli* CB9615 (Levine *et al.*, 1978; Manges *et al.*, 2008; Zhou *et al.*, 2010).

Table 1. Characteristics of *E. coli* strains selected for the preliminary studies

Strain	Characteristics	Source
ATCC 25922	Wild-type, clinical, class I	Labema/Microbiologics Inc., USA
BAA1161	Wild-type, uropathogenic, class II, serotype O17:K52:H18	ATCC, American Type Culture Collection
BW25113	Wild-type, clinical, class I	National BioResource Project (NBRP), Japan
CB9615	Wild-type, enteropathogenic, class II, similar clonal to enterohaemorrhagic, serotype O55:H7	Patrick Fach, Sabine Delannoy, ANSES, France
E2348	Wild-type, enteropathogenic, class II, serotype O127:K63:H6	Reference Microbiology Services, UK
JW5503	TolC-deleted mutant strain (parental strain: BW25113)	National BioResource Project (NBRP), Japan, (Keio Collection)
MG1655	Wild-type, class I	Prof. Karina Xavier, Instituto Gulbenkian de Ciência, Portugal

3.2.2. Chemicals and media

1-(1-naphthylmethyl)-piperazine (NMP), carbonyl cyanide 3-chlorophenylhydrazone (CCCP), Hoechst 33342 (H3342), mefloquine, phenylalanine-arginyl β-naphthylamide (PAβN), piperacillin sodium salt (PIP) and thioridazine were obtained from Sigma-Aldrich (Germany). Ciprofloxacin HCl (CIP) was purchased from ICN Biomedicals Inc. (USA), ofloxacin (OFX) was bought from MP Biomedicals, LLC. (USA) and tetracycline HCl (TET) was supplied by Calbiochem (China). Dimethyl sulfoxide (DMSO) was obtained from Merck KGaA (Germany), cation-adjusted Mueller-Hinton broth (CAMHB), Mueller-Hinton agar (MHA) and Lysogeny broth (LB) were purchased from Becton Dickinson (USA) and 0.9% saline solution, phosphate-buffered saline (PBS), 5M NaOH and 2 mg/ml kanamycin stock solution were prepared in-house.

3.2.3. H33342 accumulation assay

In the first part of the series of Hoechst 33342 (H33342) accumulation assays, all seven *E. coli* strains (Table 1) were inoculated to 10 mL of LB broth and grown overnight (16–20 h) at 37°C with shaking (200 rpm). On the next day, overnight cultures were inoculated to a fresh LB broth at a 1:100 dilution and grown until an optical density (OD) at 600 nm of 0.5–0.6 was reached. Prior to the actual H33342 accumulation assay, the growth rates of all seven *E. coli* strains were determined and the strains with similar growth rates were grouped together and inoculated at the same time to facilitate the workflow (see Appendix 1). Thus, all seven *E. coli* strains reached the desired OD around the same time. Next, bacterial cells were harvested by centrifugation at 4,000 g for 5 minutes (Centrifuge 5810R, Eppendorf), re-suspended in 10 mL of PBS and adjusted to an OD at 600 nm of 0.1–0.2 by preparing 1:5 dilution in PBS.

For H33342 accumulation assay, procedures described by Coldham *et al.* (2010) were followed. In the assay, *E. coli* JW5503 was used as a positive control (maximum H33342 accumulation). An aliquot of 180 µL of adjusted bacteria suspension was dispensed in each well (7 replicates) of a black-bottomed, 96-well plate (ViewPlate®-96 F TC, PerkinElmer). H33342 working solution (25 µM) was prepared in PBS using the stock of

17.8 mM and 20 µL of it was added to the wells containing bacteria suspension, resulting in the final concentration of 2.5 µM per well. Plates were covered with aluminum foil and carefully agitated in the Mini-Shaker (Biosan) for 5 minutes (500 rpm). Fluorescence measurements (kinetics of H33342 accumulation) were taken on Varioskan LUX (Thermo Fisher Scientific) every 5 minutes up to completion of 30 minutes using excitation and emission wavelengths of 355 and 460 nm, respectively. During readings, the plate was incubated at 37°C in Varioskan LUX. As a note, there was a lag-time of approximately 10 minutes between the addition of H33342 working solution onto the 96-well plate and the fluorescence measurement and hence the first measurement point already presents a relatively high fluorescence (data not shown) and the results reported after 30 minutes of incubation are actually presenting the intracellular H33342 accumulation of about 40 minutes.

For the follow-up study, to better evaluate the contribution of EPs in each *E. coli* strain, five EPIs were assessed in H33342 accumulation assay: PAβN, CCCP, NMP, mefloquine and thioridazine. For each EPI only one concentration was tested for all seven *E. coli* strains, based on the literature findings: CCCP at 2.0 µg/ml (Coldham *et al.*, 2010), PAβN at 50 µg/ml (Hirakata *et al.*, 2009), NMP at 100 µg/ml (Schumacher *et al.*, 2006), mefloquine at 20 µg/ml (Vidal-Aroca *et al.*, 2009) and thioridazine at 10 µg/ml (Rodrigues *et al.*, 2008). CCCP, NMP and mefloquine were dissolved in DMSO and PAβN and thioridazine in ultrapure water, the solutions were filter-sterilized either with Nylon 0.2 µm filter (PALL Life Sciences) or with PES 0.2 µm filter (VWR Internationals) and stored in the freezer at -20°C.

The assay followed the same protocol as H33342 accumulation assay described above with some modifications. Aliquots of 3.0 mL of adjusted bacteria suspensions were transferred into tubes followed by the addition of 7.5 µL of each EPI and the incubation at 37°C for 15 minutes prior to the plating. Additionally, eight replicates were performed per *E. coli* strain and per EPI. Strain with no EPI (referred as “untreated”) and heated strain were included as controls. However, the final results were plotted as a relative percentage of H33342 accumulation measured for untreated *E. coli* JW5503 and the increase in the intracellular H33342 accumulation potentiated by EPI was compared to

the intrinsic H33342 accumulation value. The main drawback of this method to study the efflux activity in the presence of EPI is that some EPIs can possess autofluorescence and thus interfere with the measurement, resulting in a false steady-state level of H33342 accumulation (Venter *et al.*, 2015). This possibility was excluded by carrying out a preliminary assay which confirmed that EPIs did not cause a significantly higher or lower fluorescence than that of the medium (PBS) and H33342 alone, indicating that only one control for background subtraction was needed to be included in the assay plates.

In the dose-response study eight different concentrations of two EPIs, CCCP and mefloquine, were studied in *E. coli* JW5503. The concentration range followed 2-fold serial dilutions as such: the concentration which was 2-fold dilutions higher than the MIC value of EPI was the highest concentration within the range and the concentration which was 64-fold dilutions lower than the MIC value was the lowest. Based on the literature findings, the MICs of CCCP and mefloquine are 10 μg/ml and 32 μg/ml (Kunin and Ellis, 2000; Viveiros *et al.*, 2005). After defining the optimal concentration for both EPIs, these same concentrations were tested in six remaining *E. coli* strains to verify whether the strains respond to EPIs at these concentrations. Assays were conducted using the same protocol as H33342 accumulation assay in the presence of EPIs, with three replicates.

3.2.4. Broth microdilution method for antibacterial susceptibility testing

The MIC is understood as the lowest concentration of an antibacterial agent that prevents visible bacterial growth (CLSI, 2015). In addition to the visual inspection, the inhibition of bacterial growth was measured using Multiskan Go plate reader (Thermo Fisher Scientific) and the lowest concentration which resulted in ≥.90% inhibition of bacterial growth was considered as the MIC value. The MIC values of four ATBs, CIP, OFX, TET and PIP, and two EPIs, CCCP and mefloquine, against four *E. coli* strains, ATCC 25922, BW25113, BAA1161 and JW5503, were determined according to the broth microdilution method for antibacterial susceptibility testing outlined by CLSI (2015). The concentration ranges tested for *E. coli* ATCC 25922 followed the approach where the highest concentration was 8-fold dilutions higher than the highest value of the MIC range defined by CLSI (2018) and the lowest concentration was 4-fold dilutions lower than the lowest

value of this MIC range. As an example, the MIC Quality Control range for TET is defined as 0.5–2 μg/ml, thus the range of concentrations tested varied from 0.125 to 16 μg/ml. The concentration ranges used for determining the MIC values of four ATBs and two EPIs for all four *E. coli* strains are presented in Appendix 2.

ATB and EPI stock solutions were prepared at the concentration of 200 times the highest concentration within the range to be tested (see Appendix 2). All ATBs were dissolved in ultrapure water, except OFX which was prepared in 1M NaOH. All solutions were filter-sterilized with PES 0.2 μm filter (VWR Internationals) followed by storage in the freezer (-20°C). Two-fold serial dilutions including eight different concentrations of ATB or EPI were prepared in strip tubes (Corning Incorporated) and stored in the freezer (-20°C). On the assay day, the dilution samples were prepared in microtiter cluster tubes (Simport) at a 1:100 dilution in CAMHB. For both minimal and maximum growth control samples 5 μL of the solvent (used for dissolving ATB or EPI) and for the positive control sample 5 μL of CIP (at the concentration of 200 times its MIC value) was added in CAMHB at a 1:100 dilution.

Bacterial growth was initiated on the day before the assay by preparing an overnight culture on MHA plate (except *E. coli* JW5503 which was grown on LB agar plate with 25 μg/ml of kanamycin), followed by incubation at 37°C for 16–20 hours. On the assay day, one colony of bacteria from the MHA plate was transferred into 5 mL of sterile saline solution and the turbidity was measured with the DEN-1 densitometer (Biosan). Bacteria suspension was adjusted to a concentration of $1x10^6$ CFU/mL in CAMHB and an aliquot of 100 μL was transferred to each well of a clear 96-well Nunc plate (Thermo Fisher Scientific). Later, 100 μL of diluted ATB or EPI was added and the final bacteria concentration of $5.0x10^5$ CFU/mL was obtained. For each dilution and control sample there were three replicates on the plate. Absorbance was measured at time points 0, 4, 7 and 24 hours using Multiskan Go plate reader (Thermo Fisher Scientific). Plates were incubated at 37°C with shaking (500 rpm) at Thermo-Shaker (PST-60HL-4, Biosan). Unless otherwise stated, MIC assays were performed in duplicates and at least two individual assays were expected to result in the same MIC value. The MIC value

determination was necessary to be carried out to define the concentration range to be tested in the checkerboard assays.

3.2.5. The checkerboard assay by Biomek i7 Automated Workstation

Preliminary experiments were conducted with four different combinations of ATB and EPI for each *E. coli* strain shown in Table 2. The results were analyzed and only the combinations which showed statistically significant decrease in the intrinsic MIC value of ATB were selected for further testing in the checkerboard assays. Nine concentrations of OFX and PIP and five concentrations of CCCP and mefloquine were tested on a clear 96-well Nunc plate (Thermo Fisher Scientific), using Biomek i7 Automated Workstation (Beckman Coulter). Each well had a unique combination of ATB and EPI concentrations (see Figure 7 for further details), following guidelines from previous studies (Lomovskaya *et al.,* 2001; Ohene-Agyei *et al.,* 2014; Coelho *et al.,* 2015). A crucial difference to the antibacterial susceptibility testing is the number of replicates per plate as in the checkerboard assay there is only one replicate for each ATB–EPI concentration combination. During the protocol optimization, one ATB–EPI combination was run in triplicates using Biomek i7 Automated Workstation in parallel with one replicate plate which was manually prepared. The results from both methods were similar, confirming that the use of the automated liquid handling was acceptable (see Appendix 3). In addition, a relatively small standard deviation between three plates prepared by Biomek i7 Automated Workstation (plate-to-plate variability) justified the use of only one plate at a time for the following runs.

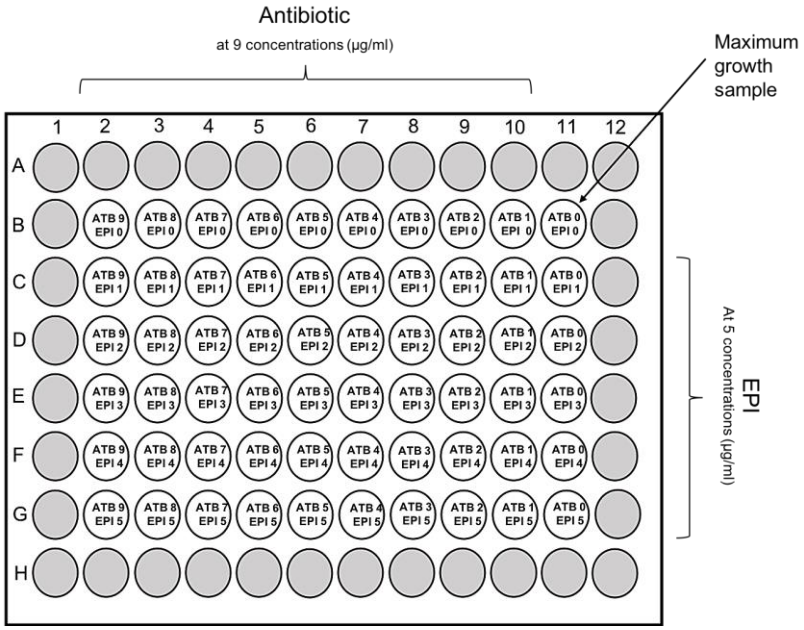

Figure 7. Layout of the destination plate, a clear 96-well Nunc plate (Thermo Fisher Scientific). Antibiotic (ofloxacin or piperacillin) is serially diluted from left to right and EPI (CCCP or mefloquine) from bottom to top, the first row containing only ATB and the last column containing only EPI. The maximum growth sample has no ATB or EPI. Grey wells contain cation-adjusted Mueller-Hinton broth only.

The source plate including 2-fold serial dilutions of ATB (on the row) and EPI (on the column) was prepared manually. Exceptionally, the concentration range tested for mefloquine did not follow 2-fold serial dilutions (see Table 2). For OFX, mefloquine and CCCP the concentration of the stock solution was 100 times the highest concentration within the range to be tested. Due to solubility issues of PIP, the concentration of the stock solution was only 40 times the highest concentration within the range tested. This was compensated in the Biomek i7 protocol by transferring a higher volume of PIP (5 µL) from the source plate to the destination plate.

Table 2. Combinations of ATB and EPI used in the checkerboard assays

Strain	ATB and EPI (µg/mL)			
	OFX + Mefloquine	OFX + CCCP	PIP + Mefloquine	PIP + CCCP
E. coli BW25113	**ATB**: 0.06 – 0.03 – 0.015 – 0.0075 – 0.00375 – 0.0019 – 0.00095 – 0.00048 – 0.00024 – 0 **EPI**: 16 – 12 – 8 – 6 – 4 – 0	**ATB**: 0.06 – 0.03 – 0.015 – 0.0075 – 0.00375 – 0.0019 – 0.00095 – 0.00048 – 0.00024 – 0 **EPI**: 10 – 5 – 2.5 – 1.25 – 0.625 – 0	**ATB**: 4 – 2 – 1 – 0.5 – 0.25 – – 0.125 – 0.0625 – 0.0313 – 0.0156 – 0 **EPI**: 16 – 12 – 8 – 6 – 4 – 0	**ATB**: 4 – 2 – 1 – 0.5 – 0.25 – 0.125 – 0.0625 – 0.0313 – 0.0156 – 0 **EPI**: 10 – 5 – 2.5 – 1.25 – 0.625 – 0
E. coli BAA1161	**ATB**: 0.12 – 0.06 – 0.03 – 0.015 – 0.0075 – 0.00375 – 0.0019 – 0.00095 – 0.00048 – 0 **EPI**: 16 – 12 – 8 – 6 – 4 – 0	**ATB**: 0.12 – 0.06 – 0.03 – 0.015 – 0.0075 – 0.00375 – 0.0019 – 0.00095 – 0.00048 – 0 **EPI**: 10 – 5 – 2.5 – 1.25 – 0.625 – 0	**ATB**: 1024 – 512 – 128 – 64 – 32 – 16 – 8 – 4 – 2 – 0 **EPI**: 16 – 12 – 8 – 6 – 4 – 0	**ATB**: 1024 – 512 – 128 – 64 – 32 – 16 – 8 – 4 – 2 – 0 **EPI**: 10 – 5 – 2.5 – 1.25 – 0.625 – 0

Mixing of ATB and EPI on the destination plate occurred by Biomek i7 Automated Workstation. Two microliters of ATB (expect PIP) and EPI were transferred from the manually prepared source plate to the destination plate. Prior to the transfer, Biomek i7 Automated Workstation was used to dispense 96 µL of CAMHB into each well of a clear 96-well Nunc plate (Thermo Fisher Scientific). 100 µL of bacteria suspension at a concentration of $1x10^6$ CFU/mL (prepared in the same manner as in the antibacterial susceptibility testing described above) was added manually afterwards in the biosafety class II cabinet. Absorbance was measured at time points 0, 4 and 24 hours using Multiskan Go plate reader (Thermo Fisher Scientific) and between readings the plate was incubated at 37°C with shaking (500 rpm) at Thermo-Shaker (PST-60HL-4, Biosan). Depending on the combination of ATB–EPI tested, assays were repeated from 3 to 5 times.

3.2.6. Data analysis

Instead of showing the kinetics within 30 minutes, results of H33342 accumulation assays were plotted as the mean of two individual assays ± SD (or as boxplots, see below) after 30 minutes of incubation, considering that the steady-state level of H33342 accumulation measured for *E. coli* JW5503 was the maximum. The performance of H33342 accumulation assay was assessed by quality parameters (Z'-factor, S/N and S/B) and it was concluded that the best performance was achieved after 30 minutes of incubation (the table of quality parameters and the equations for calculating Z'-factor, S/N and S/B are shown in Appendix 4). For assessing the contribution of EPs to the results obtained from the preliminary H33342 accumulation assay, the change in the intracellular H33342 accumulation potentiated by EPI was related to the intrinsic H33342 accumulation values and plotted as percentages. The results of checkerboard assays were expressed as the mean inhibition (%) in each well, using both numeric values and a color coding along green–red -scale. Additionally, the MIC values of ATB in the presence of increasing concentration of EPI were summarized in the table format to better demonstrate the impact of increasing concentration of EPI on the intrinsic MIC value of ATB (see Table 4). When EPI and ATB are combined together, the MIC value of ATB is anticipated to be comparable to that of *E. coli* JW5503 (Venter *et al.*, 2015). The equations used for

calculating both the modulation factor (MF) and the fractional inhibitory concentration (FIC) are presented below (Coelho *et al.*, 2015). Modulation factor indicates the fold change in the intrinsic MIC value, at least 4-fold decrease considered to be statistically significant (Bohnert and Kern, 2005; Schumacher *et al.*, 2006; Coelho *et al*., 2015). Fractional inhibitory concentration is used as an indicative of synergism, FIC < 0.25 interpreted as a synergistic effect between ATB and EPI.

$$MF = \frac{\text{MIC antibiotic}}{\text{MIC combination}} \quad (1)$$

$$FIC_{\text{antibiotic}} = \frac{\text{MIC combination}}{\text{MIC antibiotic}} \quad (2)$$

The data was analyzed using IBM SPSS Statistics, version 25. One-way ANOVA and Tukey's *post hoc* test were performed if the independent groups followed normal distribution (assessed by Shapiro-Wilk's test, $p > 0.05$) and the variances of independent groups were homogeneous (assessed by Levene's test, $p > 0.05$). If the independent groups were normally distributed but the assumption of homogeneity of variances was violated, Welch ANOVA and Games-Howell's *post hoc* test were chosen. If there were one or more independent groups which did not follow normal distribution, the data was analyzed using the non-parametric test, Kruskal-Wallis H test with a Bonferroni correction for multiple comparisons. The level of $p \leq 0.05$ was accepted as statistically significant. If data was analyzed using one-way ANOVA, the results were plotted as the mean of two individual assays ± SD. However, if the data was analyzed using Kruskal-Wallis H test, the results were plotted as boxplots, the mid-line expressing the middle value (the median) and the boxplots representing the data of two individual assays. Furthermore, the adjusted p-values (meaning that p-values were multiplied by the number of pairwise comparisons) were reported when data was analyzed using the non-parametric test.

3.3. Results

3.3.1. H33342 accumulation assay shows differences between *E. coli* strains in terms of their intrinsic efflux activities

The aim of the H33342 accumulation assay was to assess the intrinsic efflux activity of *E. coli* strains. There are several direct and indirect methods to study efflux activity: one of the indirect methods is to measure the level of fluorescent DNA-intercalating dye (e.g. H33342 which is a substrate of EPs) accumulated by bacterial cells (Blair and Piddock, 2016). In this method higher intracellular accumulation of fluorescent probe means lower efflux activity. In respect of the objectives defined in our study, the E. *coli* strain with the highest efflux activity is the most desirable choice for the screening of novel EPIs.

Statistical analysis showed significant differences between *E. coli* strains in terms of their intrinsic efflux activities (Figure 8). It was assumed that wild-type pathogenic *E. coli* strains, i.e. uropathogenic *E. coli* BAA1161 and enteropathogenic *E. coli* E2348 and *E. coli* CB9615, express EP systems at a higher extent than wild-type non-pathogenic *E. coli* strains as there is evidence of EPs playing a role in virulence, pathogenicity and AMR (Piddock, 2006). However, as an enteric bacterium, which survives under the presence of high concentration of bile salts, it was expected that all *E. coli* strains would express EP systems at the basal level and thus show some efflux activity (Thanassi *et al.*, 1997; Alcalde-Rico *et al.*, 2016). However, the lowest efflux activity was observed for *E. coli* E2348, BW25113 and MG1655, while the highest efflux activity was detected for *E. coli* ATCC 25922 of all wild-type *E. coli* strains.

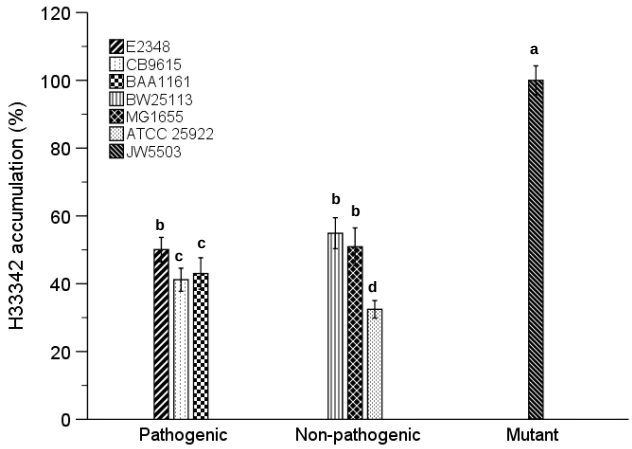

Figure 8. Steady-state level of H33342 (2.5 μM) accumulation after 30 minutes of incubation at 37 °C. The results are presented as the mean of two individual assays (n = 14) ± SD and expressed as a relative percentage of H33342 accumulation obtained for *E. coli* JW5503. Pairwise comparisons were carried out using one-way ANOVA and Tukey's *post hoc* test. The statistical significance level of $p \leq 0.05$ was used and the same letter above bars indicates that there was no statistically significant difference ($p > 0.05$).

As it was expected, the steady-state level of H33342 accumulation was significantly the highest in *E. coli* JW5503 (which carries a deficient EP, $p < 0.001$) because it is not capable of extruding H33342 out of the bacterial cells as efficiently as efflux-proficient *E. coli* strains. The mean difference of 45.1% between parental strain *E. coli* BW25113 and its derivative mutant *E. coli* JW5503 (95 % Cl: 40.3 to 49.9%) can be explained by the contribution of EPs as the gene encoding for the TolC channel is the only gene knocked out in *E. coli* JW5503, otherwise the genomes of these two strains are the same (Baba *et al.,* 2006).

3.3.2. Different classes of EPIs increase the intracellular H33342 accumulation

The data set generated in the second part of the series of H33342 accumulation assays was assumed to aid with the selection of both *E. coli* strain and EPI for the follow-up studies. The aim of the assay was to better evaluate the contribution of EPs to the findings observed in the preliminary H33342 accumulation assay and to test which EPI will lead to the highest steady-state level of H33342 accumulation and whether this same trend will be seen throughout all *E. coli* strains. Ideally, the intracellular H33342 accumulation would be similar to that measured for *E. coli* JW5503. Additionally, the EPI chosen to the follow-up studies should primarily inhibit efflux activity and not have additional

modes of action as stated by Lomovskaya *et al.* (2001). However, as previously described in the literature review, unspecific mechanisms of action have been demonstrated at least for PAβN (Matsumoto *et al.*, 2011; Lamers *et al.*, 2013; Misra *et al.*, 2015) which was one of the commercially available EPIs included in the study. Thus, the assumption of EPI not increasing the steady-state level of H33342 accumulation in *E. coli* JW5503 was very likely unmet at least with PAβN. The data set was analyzed in two different ways depending on whether the data was used to choose *E. coli* strain or EPI.

For each EPI only one concentration was tested for all seven *E. coli* strains, based on the literature findings: CCCP at 2.0 μg/ml (Coldham *et al.*, 2010), PAβN at 50 μg/ml (Hirakata *et al.*, 2009), NMP at 100 μg/ml (Schumacher *et al.*, 2006), mefloquine at 20 μg/ml (Vidal-Aroca *et al.*, 2009) and thioridazine at 10 μg/ml (Rodrigues *et al.*, 2008). In Figure 9, five EPIs within each *E. coli* strain were compared in terms of their ability to increase the intracellular H33342 accumulation. When comparing the median H33342 accumulation of five EPIs, mefloquine led to the highest median H33342 accumulation in all *E. coli* strains except *E. coli* JW5503: 115% for *E. coli* BW25113, 112% for *E. coli* MG1655, 103% for *E. coli* ATCC 25922, 119% for *E. coli* E2348, 122% for *E. coli* CB9615 and 130% for *E. coli* BAA1161, resulting in higher steady-state level of H33342 accumulation than that measured for untreated *E. coli* JW5503 (100%). Thioridazine resulted in the lowest median H33342 accumulation in all *E. coli* strains except *E. coli* E2348 and JW5503: 51% for *E. coli* BW25113, 41% for *E. coli* MG1655, 71% for *E. coli* ATCC 25922, 85% for *E. coli* CB9615 and 60% for *E. coli* BAA1161, indicating no increase in the intracellular H33342 accumulation relative to that measured in the preliminary H33342 accumulation assay for *E. coli* BW25113 and *E. coli* MG1655 (Figure 8). In terms of median H33342 accumulation, mefloquine, followed by PAβN and NMP, were the most potent EPIs at the tested concentrations.

In agreement with the previous literature findings and the suggestions made above, the maximum level of H33342 accumulation (assumed as 100%, see Figure 8) was exceeded after the addition of PAβN (Figure 9G). Interestingly, NMP, mefloquine and thioridazine had the response similar to that of PAβN and CCCP was the only EPI which did not exceed the maximum level of H33342 accumulation.

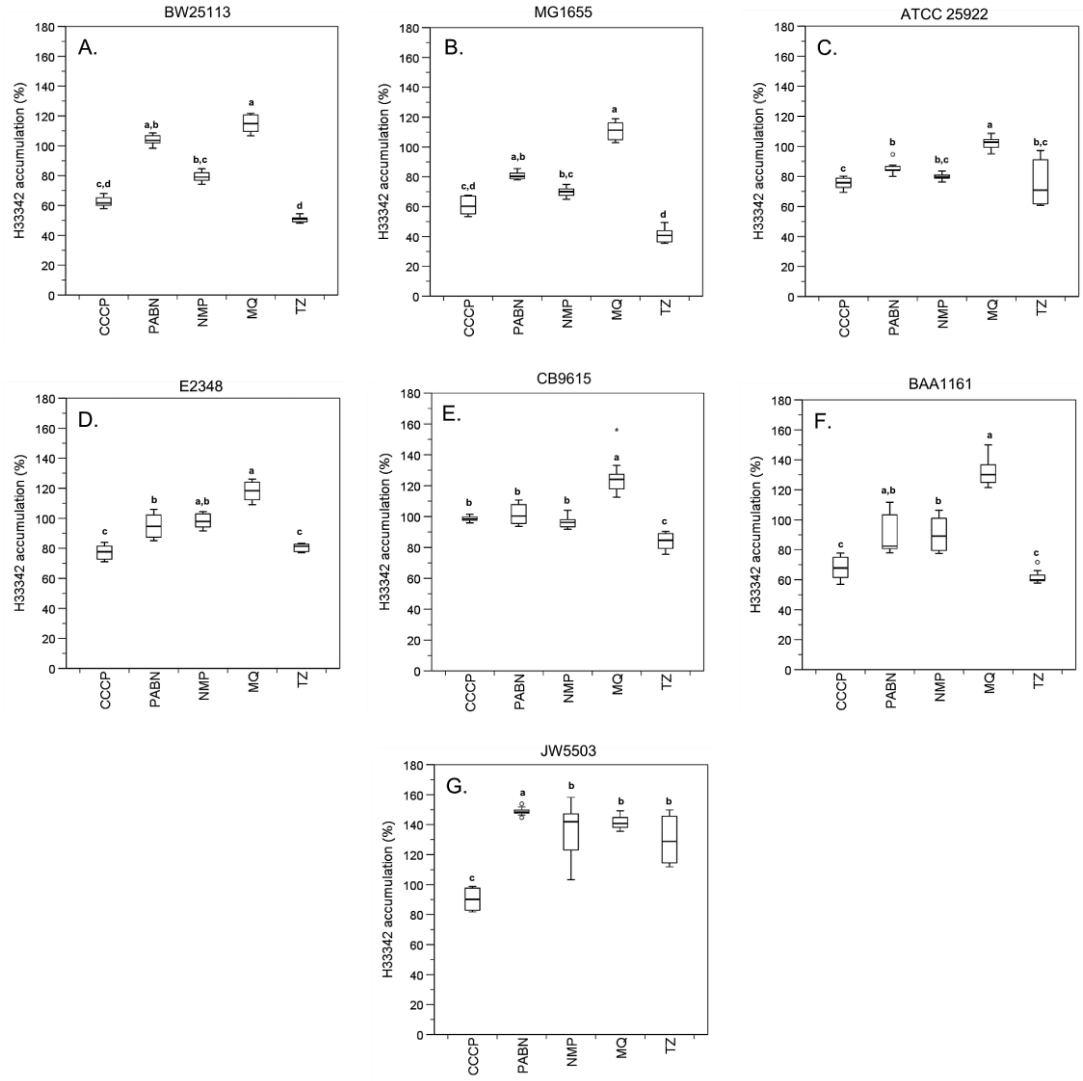

Figure 9. Steady-state level of H33342 (2.5 μM) accumulation in the presence of EPI after 30 minutes of incubation at 37 °C. The results are normalized against the maximum level of H33342 accumulation obtained for untreated *E. coli* JW5503, plotted as boxplots (n = 16) and the response to each EPI (CCCP 2.0 μg/ml, PAβN 50 μg/ml, NMP 100 μg/ml, mefloquine 20 μg/ml and thioridazine 10 μg/ml) are shown for each *E. coli* strain separately: **A.** BW25113, **B.** MG1655, **C.** ATCC 25922, **D.** E2348, **E.** CB9615, **F.** BAA1161 and **G.** JW5503. Boxplots consist of the following components: the horizontal line in the box illustrates the middle value of data and 50% of values lie within the box. The upper and lower whiskers cover the values outside the middle 50%. Outliers are shown as dots and extreme outliers as asterisks (*). Data was analyzed using Kruskal-Wallis H test and a Bonferroni correction for multiple comparisons, at a significance level of $p \leq 0.05$. The same letter above bars indicates that there is no statistically significant difference ($p > 0.05$) between EPIs. Experiment was done in duplicates with 8 replicates in each. MQ = mefloquine, TZ = thioridazine.

The magnitude of increase in H33342 accumulation was dependent on the contribution of EPs to the results obtained from the preliminary H33342 accumulation assay (Figures 8 and 10). *E. coli* BAA1161 had the highest median increase in the intracellular H33342 accumulation, independent of the EPI tested, i.e. 168% for CCCP, 257% for PAβN, 250% for NMP, 430% for mefloquine and 152% for thioridazine, followed by either *E. coli* CB9615, *E. coli* MG1655 or *E. coli* BW25113, respectively. Even though the highest median increase was obtained for *E. coli* BAA1161, it was not significantly superior compared to all *E. coli* strains in terms of increasing the steady-state level of H33342 accumulation.

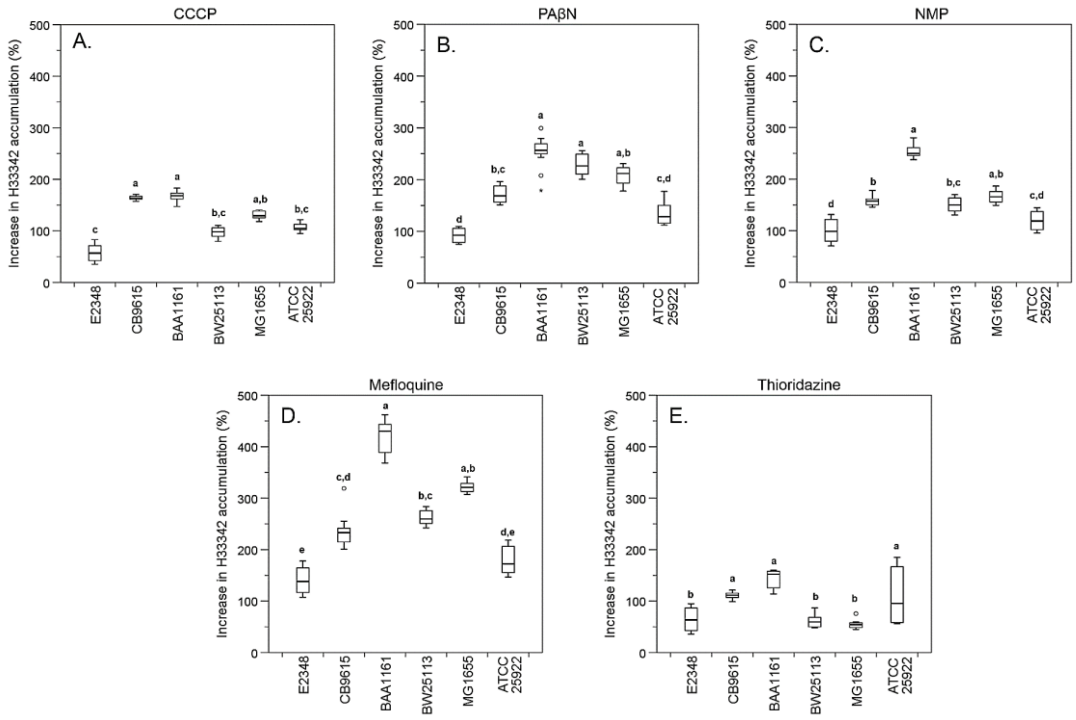

Figure 10. Increase (%) in the intracellular H33342 accumulation potentiated by EPI after 30 minutes of incubation at 37 °C, plotted as boxplots (n = 16): **A.** CCCP (2.0 μg/ml), **B.** PAβN (50 μg/ml), **C.** NMP (100 μg/ml), **D.** mefloquine (20 μg/ml) and **E.** thioridazine (10 μg/ml). Outliers are shown as dots and extreme outliers as asterisks (*). Data was analyzed using Kruskal-Wallis H test and a Bonferroni correction for multiple comparisons, at a significance level of $p \leq 0.05$. The same letter above bars indicates that there is no statistically significant difference ($p > 0.05$) between EPIs. Experiment was done in duplicates with 8 replicates in each.

3.3.3. Dose-response studies as a tool to define an optimal concentration of EPI

Two EPIs, CCCP and mefloquine, proceeded to the dose-response study (see Figure 9 for details) where eight concentrations of each EPI were tested in *E. coli* JW5503 to define an optimal concentration which would result in a similar response than that measured for untreated *E. coli* JW5503 (maximum 100%). As seen in Figure 11A, the highest concentration of CCCP classified in the same subgroup as untreated *E. coli* JW5503 (with no CCCP) was 1.25 μg/ml (99.4 ± 4.0%), meaning that there was no statistically significant difference between these two concentrations ($p = 1.0$). Concentrations higher than 1.25 μg/ml were significantly different from untreated *E. coli* JW5503 ($p < 0.001$). Interestingly, the shape of dose-response curve of CCCP was reversed in respect of what is usually seen: exceptionally, higher concentrations of CCCP resulted in lower responses. For mefloquine, two concentration ranges were required to find the concentration which was not significantly different ($p > 0.05$) from untreated *E. coli* JW5503. At higher concentration range this concentration would have been 4.0 μg/ml (119.6 ± 9.4%; $p = 0.075$) and at lower range 0.5 μg/ml (104.3 ± 6.2%; $p = 0.754$).

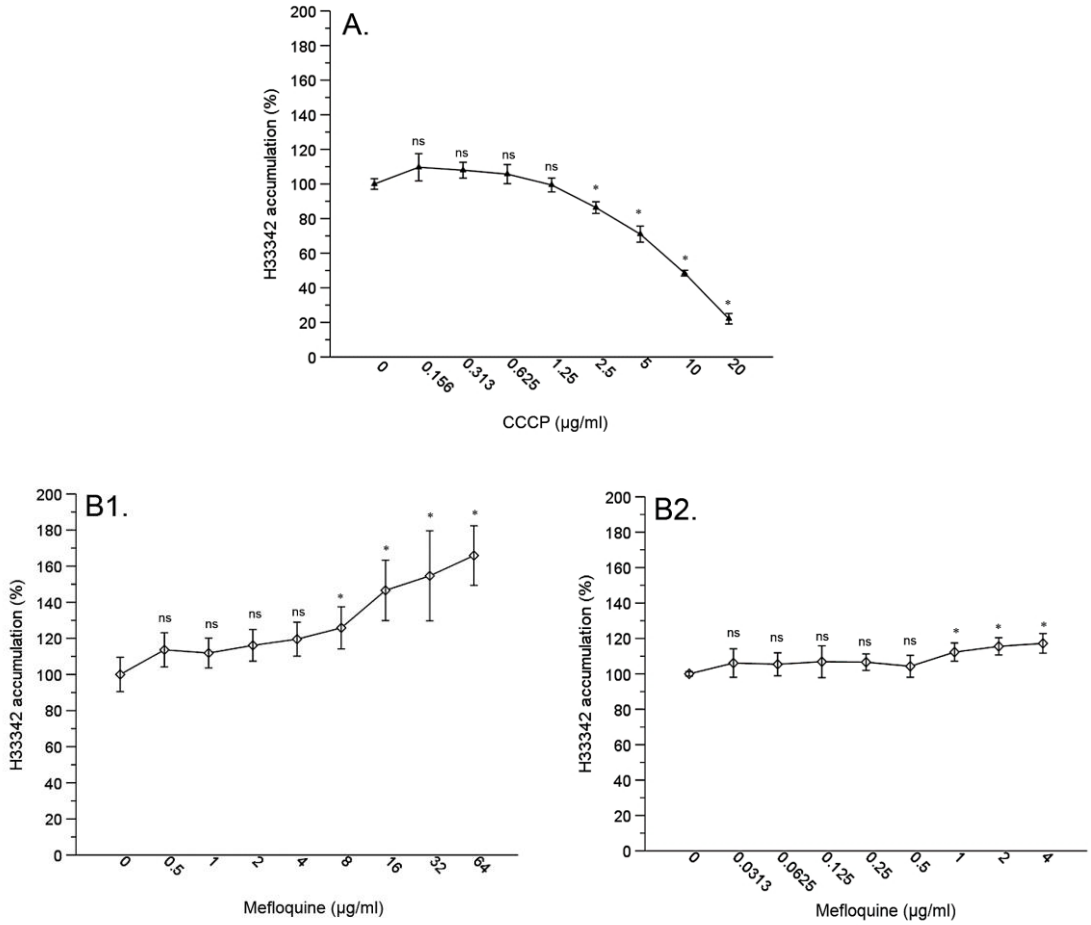

Figure 11. Steady-state level of H33342 (2.5 µM) accumulation in *E. coli* JW5503 after 30 minutes of incubation at 37°C with two different EPIs. **A.** CCCP tested from 0 to 20 µg/ml. **B1.** Mefloquine was tested from 0 to 64 µg/ml and **B2.** from 0 to 4 µg/ml. The results are expressed as the mean of two individual assays (n = 6) ± SD and plotted as a relative percentage of H33342 accumulation measured for untreated *E. coli* JW5503. The data was analyzed using Welch ANOVA and Games-Howell *post hoc* test, at a significance level of $p \leq 0.05$. Asterisk (*) above data point implies that there is statistically significant difference in the response relative to that measured for untreated *E. coli* JW5503. Ns = no significant.

In conclusion, 1.25 µg/ml of CCCP and 0.5 µg/ml of mefloquine were chosen as optimal concentrations to be further tested for six remaining *E. coli* strains. CCCP at 1.25 µg/ml resulted in the response of 70.8–92.3%, respectively (Figure 12). Although optimal concentration of mefloquine determined for *E. coli* JW5503 was 0.5 µg/ml (Figure 11B2), the same was not observed when tested in six remaining *E. coli* strains (see Appendix 5 for details). Consequently, the concentration of mefloquine was increased up to 4.0 µg/ml as this concentration did not result in extensively higher response than the maximum (100%) in *E. coli* JW5503 (117.2 ± 5.5%, Figure 11B2).

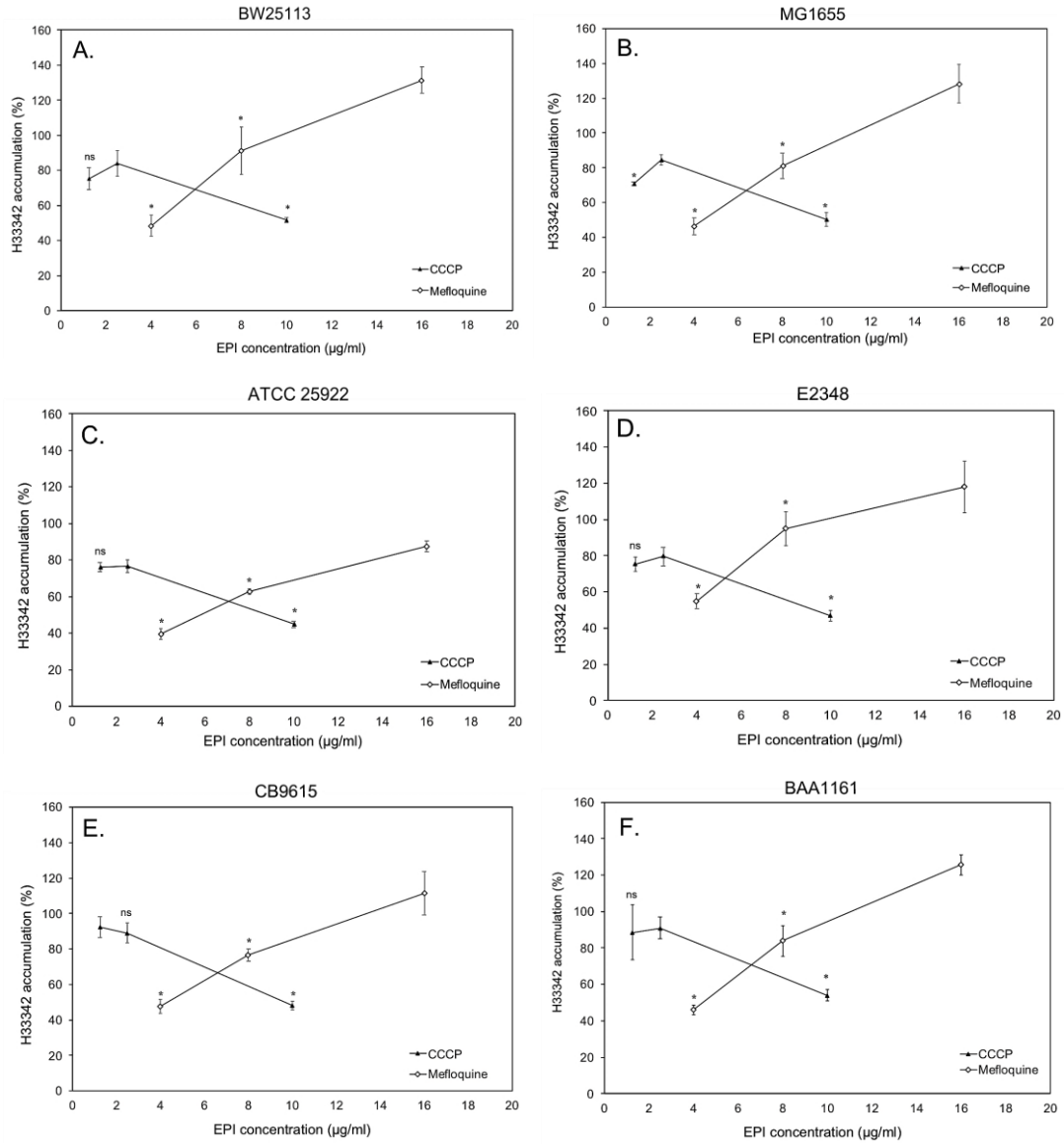

Figure 12. Steady-state level of H33342 (2.5 µM) accumulation after 30 minutes of incubation at 37°C with CCCP (1.25, 2.5 and 10 µg/ml) and mefloquine (4, 8 and 16 µg/ml) for *E. coli* **A.** BW25113, **B.** MG1655, **C.** ATCC 25922, **D.** E2348, **E.** CB9615 and **F.** BAA1161. The results are expressed as the mean of two individual assays (n = 16) ± SD and plotted as a relative percentage of H33342 accumulation obtained for untreated *E. coli* JW5503. The data was analyzed using either one-way ANOVA or Kruskal-Wallis H test depending on whether data was normally distributed or not, at a significance level of $p \leq 0.05$. Asterisks (*) above data point implies that there is statistically significant difference in the response relative to that measured for CCCP 2.5 µg/ml or mefloquine 16 µg/ml. Ns = no significant.

Overall, mean increases in the intracellular H33342 accumulation after 30 minutes of incubation with CCCP at 2.5 μg/ml were higher than those obtained with CCCP at 1.25 μg/ml. In most cases, no statistically significant difference between these two concentrations was observed ($p > 0.05$), except in *E. coli* MG1655 for which 2.5 μg/ml gave statistically significantly higher response than 1.25 μg/ml ($p = 0.004$) (Figure 12B). The decrease in response in a dose-dependent manner was also noted in six remaining *E. coli* strains as observed for *E. coli* JW5503 previously (Figures 11A and 12). Based on these findings, the concentration range chosen to be tested in the checkerboard assays included 2.5 μg/ml as the highest concentration for CCCP.

For mefloquine, the concentration of 16.0 μg/ml had significantly the highest response of all three concentrations studied here ($p < 0.05$) but the maximum level of H33342 accumulation (100%) was exceeded (Figure 12). For some *E. coli* strains, even 8.0 μg/ml of mefloquine resulted in the intracellular H33342 accumulation relatively close to the maximum level (100%), i.e. 83.8 ± 7.2% for *E. coli* BW25113, 81.1 ± 7.1% for *E. coli* MG1655, 94.8 ± 9.4% for *E. coli* E2348 and 83.9 ± 8.4% for *E. coli* BAA1161, respectively. However, as the maximum level of H33342 accumulation (100%) would be reached at some concentration between 8.0 and 16 μg/ml, further testing which included one concentration between 8.0 and 16 μg/ml was performed during the checkerboard assays.

3.3.4. The intrinsic MIC values of ATBs and the resistance to ATBs reversed by EPIs

Based on the findings illustrated in Figure 10, *E. coli* BAA1161 was selected for the antibacterial susceptibility testing as a representative for wild-type pathogenic *E. coli* strains. Within all wild-type non-pathogenic *E. coli* strains, the MIC values of four ATBs, CIP, OFX, PIP and TET, and two EPIs, CCCP and mefloquine, were determined for *E. coli* BW25113, thus allowing for comparison between parental and efflux-deficient mutant *E. coli* strains. The inclusion of *E. coli* ATCC 25922 in the antibacterial susceptibility testing was justified as *E. coli* ATCC 25922 is recommended by CLSI as a reference standard, with known MIC values for several ATBs defined by CLSI (2018).

The results of MIC value determination for four *E. coli* strains are reported in Table 3. More detailed information regarding tested concentration ranges and the number of individual assays required for the MIC value determination are provided in Appendix 2.

Table 3. MIC values (μg/ml) determined using the broth microdilution method according to Clinical and Laboratory Standard Institutes (CLSI, 2015).

E. coli strain	Compound	MIC (μg/ml)	MIC-ratio[a]	MIC-breakpoints[b]
ATCC 25922	CIP	0.0078	2	**S** ≤ 1.0; **I**: 2.0; **R** ≥ 4.0
	OFX	0.015	2	**S** ≤ 2.0; **I**: 4.0; **R** ≥ 8.0
	PIP	4	16	**S** ≤ 16; **I**: 32–64; **R** ≥ 128
	TET	0.5	2	**S** ≤ 4.0; **I**: 8.0; **R** ≥ 16
	CCCP	20	16	
	Mefloquine	32	4	
BAA1161	CIP	0.0078	2	**S** ≤ 1.0; **I**: 2.0; **R** ≥ 4.0
	OFX	0.06	8	**S** ≤ 2.0; **I**: 4.0; **R** ≥ 8.0
	PIP	512	2048	**S** ≤ 16; **I**: 32–64; **R** ≥ 128
	TET	128	512	**S** ≤ 4.0; **I**: 8.0; **R** ≥ 16
	CCCP	20	16	
	Mefloquine	32	4	
BW25113	CIP	0.0078	2	**S** ≤ 1.0; **I**: 2.0; **R** ≥ 4.0
	OFX	0.03	4	**S** ≤ 2.0; **I**: 4.0; **R** ≥ 8.0
	PIP	2	8	**S** ≤ 16; **I**: 32–64; **R** ≥ 128
	TET	0.5	2	**S** ≤ 4.0; **I**: 8.0; **R** ≥ 16
	CCCP	40	32	
	Mefloquine	32	4	
JW5503	CIP	0.0039	1	**S** ≤ 1.0; **I**: 2.0; **R** ≥ 4.0
	OFX	0.0075	1	**S** ≤ 2.0; **I**: 4.0; **R** ≥ 8.0
	PIP	0.25	1	**S** ≤ 16; **I**: 32–64; **R** ≥ 128
	TET	0.25	1	**S** ≤ 4.0; **I**: 8.0; **R** ≥ 16
	CCCP	1.25	1	
	Mefloquine	8	1	

[a] $MIC_{wild\text{-}type}/MIC_{mutant}$
[b] Clinical and Laboratory Standards Institute (CLSI, 2018)
S = susceptible, I = intermediate, R = resistant

It was expected that for *E. coli* JW5503 lower concentrations of ATBs and EPIs are sufficient to fully inhibit the bacterial growth (≥90%) because TolC-connected EP systems, which are involved with extruding a wide range of structurally unrelated compounds, are not expressed in this strain (Blair and Piddock, 2016). Consequently,

ATB, which is a substrate of TolC-connected EP systems, is retained inside the bacterial cell and obtains more easily the therapeutic concentration that fully inhibits bacterial growth. In fact, this assumption was supported by the findings made in the antibacterial susceptibility testing for *E. coli* JW5503 (Table 3). Furthermore, the pair of parental *E. coli* BW25113 and its derivative, TolC-deleted mutant *E. coli* JW5503 presented different MIC values for all four ATBs tested, indicating the contribution of EPs to the decreased susceptibility to antibacterial agents. The MICs of CIP and TET differed only by 2-fold but for OFX and mefloquine there was a 4-fold difference, for PIP an 8-fold difference and for CCCP even a 32-fold difference (Table 3).

According to the MIC-breakpoints shown in Table 3, clinically relevant uropathogenic *E. coli* BAA1161 was the only strain that was resistant to PIP and TET as their MICs were 4- and 8-fold higher than the breakpoint for being classified as "resistant". It basically means that *E. coli* BAA1161 is not inhibited by the usually achievable infection site concentrations of PIP and TET. However, *E. coli* BAA1161 was sensitive to quinolones, CIP and OFX. Although *E. coli* BAA1161 presented resistance profile towards two classes of ATBs, it is not sufficient to classify *E. coli* BAA1161 as an MDR strain based on tests conducted here. MDR is defined as a resistance profile to at least three different classes of ATBs (Richmond *et al.*, 2013). Further assessment using other classes of ATBs would be required to evaluate a possible MDR profile for this bacterial strain.

It was anticipated that the intrinsic MIC value of ATB will be decreased to the level comparable to that of *E. coli* JW5503 if EPI is introduced at a sub-inhibitory concentration (Bohnert and Kern, 2005; Opperman *et al.*, 2014; Coelho *et al.*, 2015; Venter *et al.*, 2015). Furthermore, if the intrinsic MIC value of ATB is decreased at least by 4-fold, there is statistically significant synergism between ATB and EPI (Coelho *et al.*, 2015). Based on the MIC ratios provided in Table 3, CIP was not a suitable ATB to further test the synergistic effects of ATB and EPI because the MICs of wild-type and TolC-deleted mutant *E. coli* strains differed only by 2-fold. In order to achieve statistically significant decrease in the intrinsic MIC value of ATB in the checkerboard assays, the two ATBs with the MIC ratio of at least 4-fold were chosen (Table 3). In conclusion, OFX and PIP

were selected as this criterion was met in two strains, *E. coli* BAA1161 and *E. coli* BW25113.

The checkerboard assay is recommended to be carried out at sub-inhibitory concentration of EPI to rule out the chance of antibacterial activity of the EPI itself. The combination of OFX and CCCP was first tested at the lower concentration range of CCCP, but it was noticed that not even the highest concentration of CCCP (2.5 μg/ml) succeeded to decrease the intrinsic MIC value of OFX (see Appendix 6). Thus, the concentration up to 10 μg/ml was tested even though a reversed dose-response relationship was observed in H33342 accumulation assays (Figures 11A and 12). The highest concentration included in the checkerboard assays was 16 μg/ml for mefloquine and 10 μg/ml for CCCP and these concentrations were half of their MICs defined for *E. coli* BAA1161(Table 3).

Altogether, four different ATB–EPI combinations for both *E. coli* BAA1161 and *E. coli* BW25113 were tested (see Table 2 for details). However, no decrease in the intrinsic MIC value of OFX was observed in the presence of either EPI. Thus, the combinations of OFX and both EPIs were tested only once and the results are provided in Appendix 6. In addition, the intrinsic MIC value of PIP did not change when the combinations of PIP and both EPIs were tested in *E. coli* BW25113. Any decrease was only seen when PIP was combined either with mefloquine or CCCP and the combinations were tested in *E. coli* BAA1161, the results of which are summarized in Tables 4 and 5.

Table 4. Checkerboard assay combining piperacillin with mefloquine for *E. coli* BAA1161. Average of four individual assays with 1 replicate in each. The value in parentheses indicates the fold change relative to the intrinsic MIC value of piperacillin and bold numbers show statistically significant differences, i.e. synergism between EPI and ATB. The equations for modulation factor (MF) and fractional inhibitory concentration (FIC) has been provided in *Materials and methods* and the highest MF and the lowest FIC are shown in the table format adopted from Lomovskaya *et al.* (2001).

E. coli strain	Genotype	Mefloquine MIC (µg/ml)	PIP MIC (µg/ml) in the presence of Mefloquine at conc (µg/ml) of						MF	FIC
			0	4	6	8	12	16		
BAA1161	UPEC	32	512	512	512	256 (2)	256 (2)	32 (**16**)	16	0.0625

Piperacillin (µg/ml)

Mefloquine (µg/ml)	1024	512	256	128	64	32	16	8	4	0
0	100	93	41	7	3	1	0	2	2	0
4	100	100	50	16	11	7	4	2	3	4
6	100	100	88	40	12	6	4	4	4	3
8	100	100	100	56	15	11	4	7	5	1
12	100	100	100	80	61	24	16	14	14	12
16	100	100	100	100	100	90	32	26	27	21

Table 5. Checkerboard assay combining piperacillin with CCCP for *E. coli* BAA1161. Average of five individual assays with 1 replicate in each. The value in parentheses indicates the fold change relative to the intrinsic MIC value of piperacillin and bold numbers show statistically significant differences, i.e. synergism between EPI and ATB. The equations for modulation factor (MF) and fractional inhibitory concentration (FIC) has been provided in *Materials and methods* and the highest MF and the lowest FIC are shown in the table format adopted from Lomovskaya *et al.* (2001).

Strain	Genotype	CCCP MIC (μg/ml)	PIP MIC (μg/ml) in the presence of CCCP at conc. (μg/ml) of						MF	FIC
			0	0.625	1.25	2.5	5	10		
BAA1161	UPEC	20	1024	1024	1024	512 (2)	512 (2)	32 (**32**)	32	0.0313

Piperacillin (μg/ml)

CCCP (μg/ml)	1024	512	256	128	64	32	16	8	4	0
0	100	85	27	6	3	1	4	2	1	0
0.625	100	60	31	15	12	11	11	7	7	8
1.25	100	54	31	16	13	12	12	9	10	8
2.5	100	92	53	39	35	28	15	17	16	11
5	100	100	79	74	70	58	21	27	29	24
10	100	100	100	100	100	100	72	75	70	71

A color coding along the green–red scale indicates the impact of increasing concentration of EPI on the inhibition level (%): the concentration of PIP is the same in each column of the 96-well plate but as it is seen, increasing the concentration of EPI improved the antibacterial efficacy of PIP (Tables 4 and 5). Mefloquine at the concentration of 16 μg/ml led to statistically significant decrease in the intrinsic MIC of PIP (16-fold) when averaging the results of four individual assays (Table 4). However, we expected to get at least a 4-fold decrease at the sub-inhibitory concentration of mefloquine (at 8.0 μg/ml or below) but only a 2-fold decrease was obtained at this concentration (Table 4). Nevertheless, it was concluded that meeting this criterion with mefloquine was not as crucial as when screening library compounds for possible EPIs. The results obtained here by combining mefloquine and PIP are satisfactory to fulfill the criterion as a positive control in HTS. Furthermore, mefloquine at the concentration of 16 μg/ml alone (with no ATB present, Table 4) resulted in only 21% inhibition of bacterial growth so even though this concentration is not sub-inhibitory, it is quite unlikely that antibacterial activity of mefloquine would have contributed to this synergistic effect observed between mefloquine and PIP in the checkerboard assays.

CCCP showed even higher improvement in the susceptibility of *E. coli* BAA1161 to PIP (Table 5). In fact, at the concentration of 10 μg/ml a 32-fold decrease was recorded. However, the contribution of antibacterial activity of CCCP itself to the observed synergism cannot be ruled out because the mean 71% inhibition of bacterial growth was demonstrated for the sample containing only CCCP at the concentration of 10 μg/ml (Table 5). In fact, the bactericidal effects of CCCP at higher concentrations has been reported in the literature (Kinoshita *et al.*, 1984; Sinha *et al.*, 2017). Additionally, in the dose-response study it was observed that higher concentrations of CCCP resulted in lower intracellular H33342 accumulations, most likely explained by a smaller bacterial cell population as the result of bactericidal effects of CCCP (Figures 11A and 12).

In conclusion, mefloquine at the concentration of 16 μg/ml was chosen to be used as a positive control and PIP at the concentration of 256 μg/ml as an ATB in HTS of novel EPIs. Even though mefloquine decreased the MIC value of PIP from 512 μg/ml to 32 μg/ml, a higher concentration of PIP was selected for HTS in order to identify library

compounds that are less potent than mefloquine but still have efflux inhibitory activity. In fact, a 4-fold decrease in the intrinsic MIC value was considered to be significant (Coelho *et al*., 2015), which would mean 128 μg/ml with the MIC of 512 μg/ml and 256 μg/ml with the MIC of 1024 μg/ml (in the checkerboard assays the intrinsic MIC value of PIP varied by one two-fold, see Tables 4 and 5). Thus, library compounds with no visible bacterial growth when combined with 256 μg/ml of PIP would possess efflux inhibitory activity which should be investigated further in the follow-up studies.

4 DISCUSSION

Based on the results obtained from the first part of the series of H33342 accumulation assays, *E. coli* ATCC 25922 seemed to have the highest efflux activity of all wild-type pathogenic and non-pathogenic strains as the steady-state level of H33342 accumulation and efflux activity are indirectly correlated with each other. However, when *E. coli* ATCC 25922 was treated with any of the five tested EPIs, the increase in the intracellular H33342 accumulation was not as high as for two wild-type pathogenic *E. coli* strains, *E. coli* CB9615 and *E. coli* BAA1161. For example, 2.0 μg/ml CCCP increased intracellular H33342 accumulation by 164 ± 3.8% for *E. coli* CB9615, by 167 ± 9.3% for *E. coli* BAA1161 but only by 107 ± 6.9% for *E. coli* ATCC 25922.

The hypothesis of *E. coli* ATCC 25922 not possessing as high efflux activity as *E. coli* BAA1161 was further supported by the results of antibacterial susceptibility testing which showed that the MICs of CIP, OFX and TET were only 2-fold higher than those measured for *E. coli* JW5503. A two-fold difference is not considered to be significant because this variation in the MIC value is acceptable as outlined by CLSI (2015). In contrast, *E. coli* BAA1161 showed a 2-fold, an 8-fold and a 512-fold difference in the MICs of CIP, OFX and TET relative to those obtained for *E. coli* JW5503. However, the MIC of PIP in *E. coli* ATCC 25922 was 16-fold higher than that defined for *E. coli* JW5503, but *E. coli* BAA1161 had even higher fold difference than *E. coli* ATCC 25922 (i.e. 2048-fold difference). In fact, *E. coli* BAA1161 was the only strain

that was resistant to any of the four tested ATBs and presumably the resistance to PIP and TET was mediated by enhanced efflux activity.

Above-described findings made in H33342 accumulation assays demonstrate very well the necessity of the follow-up study conducted in conjunction with EPIs because false conclusions regarding efflux activities of *E. coli* strains are easily drawn based on the results of preliminary assay. This example perfectly illustrates that the steady-state level of H33342 accumulation is the sum of both efflux and influx rates and the contribution of latter one can easily be neglected (Blair and Piddock, 2016). In fact, H33342 accumulation assay is a suitable method to assess efflux activities of isogenic but not phenotypically variable bacterial strains as they may have other structural differences as well, for example different OM permeability may lead to dissimilar H33342 influx rates. Indeed, low steady-state level of H33342 accumulation caused by impaired influx rate can easily get masked and the results of H33342 accumulation assay misinterpreted, i.e. the strain with lower OM permeability be mistakenly assumed to have higher efflux activity. In fact, this might have been the scenario with *E. coli* ATCC 25922. Unfortunately, the collection of *E. coli* strains included in the experiments here were not isogenic (except *E. coli* BW25113 and *E. coli* JW5503), meaning that this prerequisite for carrying out H33342 accumulation assay was not met. There is also another limitation regarding this method. The identical number of bacterial cells per sample was difficult to reproduce assay-to-assay and thus the adjustment within the OD range of 0.1–0.2 was used. However, H33342 used for the measurement of efflux activity is a DNA-intercalating fluorescent probe, meaning that a greater number of bacterial cells per sample and therefore, a greater number of binding sites for H33342 at the minor groove of double-stranded DNA will result in a higher intensity in the fluorescence measurement (Coldham *et al.,* 2010). This may partly explain the inter-assay deviations observed in the results.

However, choosing H33342 accumulation assay was justified as it is a quick, simple and cheap method and the obstacles associated with this assay can easily be overcome by conducting the follow-up assay in conjunction with EPIs (Coldham *et al.*, 2010; Richmond *et al.,* 2013). In the beginning of the project we did not have any knowledge

regarding intrinsic efflux activities of the seven tested *E. coli* strains and as H33342 accumulation assay has been considered to be a method with a high throughput (Blair and Piddock, 2016), we thought that it would be feasible for defining efflux activities of a large number of *E. coli* strains. Thus, valuable information regarding the phenotypes of several *E. coli* strains in terms of their efflux activities was generated in this project, enabling to discriminate between *E. coli* strains with low and high efflux activities. Afterwards, it would have been interesting to complement the obtained phenotypic data with genotypic data by RT-qPCR which quantifies mRNA expression levels of EP genes (Helaly *et al.,* 2016). In fact, a combined phenotypic (antibacterial susceptibility testing and checkerboard assay) and genotypic (RT-qPCR) approach to detect efflux-mediated resistance in MDR clinical isolates has been used (Mesaros *et al.,* 2007; Helaly *et al.,* 2016). Additionally, knowing the gene expression profile of EP subtypes in each *E. coli* strain might have helped in terms of interpreting the results of checkerboard assays discussed below. However, for the purposes of this study, we considered that H33342 accumulation assay was sufficient to identify *E. coli* BAA1161 as a strain with a high efflux activity (the finding which was further supported by antibacterial susceptibility testing and checkerboard assays).

As already discussed in the literature review, PAβN is known to alter the OM permeability and this secondary effect of PAβN is greatly amplified in efflux-deficient strain (Matsumoto *et al.*, 2011; Lamers *et al.*, 2013; Misra *et al.*, 2015). Thus, the response of NMP, mefloquine and thioridazine similar to that of PAβN in the H33342 accumulation assays may be an indicative of additional unspecific modes of action or the inhibitory activity towards EP systems other than TolC-connected EPs. Indeed, there is some evidence of phenothiazines affecting the plasma membranes of both mammalian and bacterial cells and mefloquine damaging the bacterial cell envelope and releasing DNA into the external medium (Kunin and Ellis, 2000; Amaral *et al.*, 2010). To date, there are no studies which would have proven that NMP alters the OM permeability, the activity of which could be easily studied by nitrocefin hydrolysis assay (Lomovskaya *et al.*, 2001; Ohene-Agyei *et al.*, 2014; Opperman and Nguyen, 2015). For PAβN it has been shown that it primarily inhibits AcrAB and AcrEF transporters of *E. coli* at lower concentrations and starts interfering with the OM permeability at higher concentrations

(Matsumoto *et al.*, 2011; Misra *et al.*, 2015). In TolC-deleted *E. coli* strain the impact on the OM permeability was already seen at the concentration of 4 μg/ml (Matsumoto *et al.*, 2011). On the contrary, when PAβN was tested up to 20 μg/ml no clear effects on the OM permeability were demonstrated in efflux-proficient *E. coli* strain (Misra *et al*., 2015). Following the same approach and testing mefloquine at lower concentrations down to 0.0313 μg/ml in *E. coli* JW5503, mefloquine might have exerted its action primarily via the pump inhibition at the concentration of 0.5 μg/ml. Unfortunately, the other six *E. coli* strains we tested did not respond to mefloquine at this concentration. The results obtained here confirmed that there are safety-related challenges associated with the EPIs described in the literature. Even though there is not a perfect EPI yet commercially available according to the criteria list described by Lomovskaya *et al.* (2001), we tried to select the best EPI in terms of its ability to potentiate the bacterial susceptibility to ATBs.

Another interesting finding was the dose–response relationship of CCCP that differed from the dose-response relationship obtained for mefloquine. This observation may be explained by the bactericidal effects of CCCP at higher concentrations, only >50% of bacterial cells were recovered after an hour of incubation with CCCP at the concentration corresponding to half of its MIC (Sinha *et al.*, 2017). In fact, the highest concentration (20 μg/ml) tested in dose-response studies was 16-fold higher than the MIC of CCCP defined for *E. coli* JW5503 but exactly the same as the MIC of CCCP for *E. coli* BAA1161 so interference with the bacterial cell viability seems to be a very likely explanation for the observations made in the dose-response studies.

E. coli is known to have a relatively short generation time (approximately 20 minutes under favorable conditions) and during 15 minutes' pre-incubation time and extra 10 minutes prior to the first fluorescence measurement on Varioskan LUX, one doubling of bacterial cell population has already taken place (Tortora *et al.*, 2016). Theoretically, while the bacterial cell count is doubled in samples with low concentrations of CCCP within 20 minutes, the addition of CCCP at high concentrations either stops bacterial growth and re-starts it after some lag period or bacterial growth is stopped completely (Kinoshita *et al.*, 1984). Either way, presumably there will be dissimilarities in the bacterial cell count in low and high concentration samples when the fluorescence

measurement is initiated. As previously described, H33342 accumulation assay is based on the transition in the maximum emission wavelength and increase in the fluorescence intensity when H33342 is intercalated with DNA (Coldham *et al.*, 2010; Richmond *et al.*, 2013). The higher the number of binding sites in DNA, the higher the amount of H33342 intercalated and thus the signal detected in the fluorescent measurement is stronger. Whether bacterial growth is affected by CCCP, the size of bacterial cell population and the total amount of DNA will be smaller, meaning that less H33342 will be accumulated by bacterial cells, resulting in a lower signal in the fluorescence detection (Seigel and Campbell, 2004).

However, it was shown that cytotoxicity of CCCP was not only concentration- but also time-dependent and evident cytotoxicity was only seen after 2 hours of incubation with 100 μM (20 μg/ml) of CCCP (Yang *et al.*, 2001). Additionally, in the study by Coldham *et al.* (2010) where the H33342 accumulation assay was originally introduced, a reversed dose-response relationship for CCCP at the tested concentration range (0.1–10 μM, respectively) was not demonstrated as we did here. However, the highest concentration tested by these authors corresponded to 2.0 μg/ml that was the same concentration which we selected to the preliminary H33342 accumulation assay. In fact, a reversed dose-response relationship was observed only after including higher concentrations than 2.0 μg/ml in our assays, thus making inter-assay comparisons regarding this phenomenon impossible as the study by Coldham *et al.* (2010) did not show any data at a higher concentration range. We could not find any other study aiming to detect the influence of increasing concentration of CCCP in the literature to compare the results to ours.

The results of the checkerboard assays suggest that resistance of *E. coli* BAA1161 to PIP observed in the antibacterial susceptibility testing is due to an enhanced efflux activity. Additionally, PIP seemed to be a good substrate of TolC-connected EPs because the MIC ratio of 2048 (the ratio of $MIC_{wild\text{-}type}$ and MIC_{mutant}) was obtained. When *E. coli* BAA1161 was exposed to 10 μg/ml of CCCP, the intrinsic MIC value of PIP decreased by 32-fold and when combined with 16 μg/ml of mefloquine, a 16-fold decrease in the intrinsic MIC value of PIP was observed. This represents a shift from resistant ATB profile to intermediate, respectively. As the bacterial susceptibility to PIP was not

completely restored (the MIC of PIP should have reduced to 16 μg/ml or less when combined with EPI), this finding could be interpreted as an indicative of combinatorial resistance mechanisms, e.g. degradation of ATB by hydrolysis, decreased OM permeability and structural modifications in the target site, meaning that enhanced efflux activity only partly contributed to the overall resistance (Kumar and Varela, 2013). The probability that the synergism detected for PIP and mefloquine (a 16-fold decrease) was due to antibacterial activity of mefloquine itself is quite unlikely as only 21% of inhibition of bacterial growth at the concentration of 16 μg/ml was measured. Additionally, mefloquine has shown only a poor antibacterial efficacy towards GNB (Kunin and Ellis, 2000), which may be explained by the extrusion of mefloquine out of the bacterial cells if efflux inhibitory activity of mefloquine is based on the competitive inhibition (meaning that mefloquine competes with antibacterial agents to be pumped out via EPs).

Interestingly, *E. coli* BAA1161 was not resistant to OFX and thus there was no efflux-mediated resistance to be reversed by combining either EPI with OFX in the checkerboard assays (see Appendix 6). Based on the results obtained from the H33342 accumulation assays and a 16- to 32-fold decrease in the intrinsic MIC of PIP demonstrated in the checkerboard assays, *E. coli* BAA1161 seemed to have an increased efflux activity as concluded above. Still, the intrinsic MIC of OFX, which is also a substrate of AcrAB-TolC tripartite protein complex (Oethinger *et al.*, 2000), was not affected, suggesting that OFX and PIP are pumped out of the bacterial cells via a dissimilar range of EP systems. In fact, based on the results of H33342 accumulation assay carried out in *E. coli* JW5503, it seemed that mefloquine has inhibitory activity towards other EP systems as well because only TolC-connected EPs were deleted in *E. coli* JW5503 and EP systems belonging to other superfamilies, such as the MFS and SMR, are known to be expressed in *E. coli* as well (Li ans Nikaido, 2004). Hypothetically, the expression level of EPs responsible for extruding PIP is elevated in *E. coli* BAA1161, resulting in a high intrinsic MIC value of PIP. Meanwhile, there is no impact on the MIC value of OFX as this antibacterial agent is not a substrate of the same range of EP systems overexpressed in *E. coli* BAA1161. Consequently, reversing resistance of *E. coli* BAA1161 to PIP, but not to OFX, in the presence of mefloquine could be explained by the inhibition of overexpressed EP systems which are exclusively involved with extruding PIP out of the

bacterial cells. Defining the profile of (over)expressed EP systems in *E. coli* BAA1161 by RT-qPCR would confirm this hypothesis.

PIP is formulated in its salt form (sodium salt) and there is a carboxylic acid in the molecular structure of OFX that is ionized at physiological pH (DrugBank, 2018). Thus, PIP and OFX are hydrophilic in nature and permeate the OM mainly by the porin-mediated pathway (Delcour, 2009). The ratio between uncharged and charged forms of OFX is dependent on the external pH relative to the pKa of OFX and the lipid-mediated pathway can also be utilized when OFX is in its uncharged state. Furthermore, a third cellular uptake pathway has been proposed for OFX (Chapman and Georgopapadakou, 1988). Fluoroquinolones, such as OFX, work as self-promoters in a similar manner as aminoglycosides and cationic peptides, meaning that fluoroquinolones improve their own cellular uptake by destabilizing the OM structure and thus readily reach their intracellular targets. β-lactams, such as PIP, permeate the OM mainly via OmpF porins as mentioned above (Nikaido, 2003). However, it was shown that PIP has relatively slow permeation rate through OmpF porins due to its large size and its negligible interactions with the constriction area inside the OmpF channel (Danelon *et al.*, 2005). In conclusion, the influx rate of OFX may be higher than that of PIP as there are three pathways in total which OFX can utilize for its cellular uptake. In contrast, the only pathway exploited by PIP is not working efficiently due to its high molecular weight, meaning that PIP has intrinsically more retarded influx to the interior of bacterial cells than OFX.

Even though both antibacterial agents are relatively hydrophilic, logP value, that is the logarithm of the ratio of uncharged drug partitioned between the organic and aqueous phases, is slightly higher for PIP than for OFX (0.3 and -0.39; DrugBank, 2018). The hydrophobic trap within the DBP of the AcrB porter domain consists of several aromatic side chains and thus especially lipophilic drugs are preferred by the AcrAB transporter (Nikaido *et al.*, 1998; Murakami *et al.*, 2006; Lim and Nikaido, 2010). PIP may have a higher affinity to the AcrAB transporter than OFX, thus resulting in a higher efflux rate. However, in order to confirm this hypothesis, the kinetic parameters of the efflux process, such as K_m (the concentration required for the half-maximum velocity) and V_{max} (the maximum rate of efflux), should be defined for both PIP and OFX because the MIC ratio

itself is not a sufficient measure for efflux efficiencies (Lim and Nikaido, 2010). In conclusion, lower MIC ratio of OFX compared to PIP in *E. coli* BAA1161 (8 versus 2048) could be explained by OFX having higher influx and lower efflux rates than PIP due to multiple cellular uptake pathways and lower affinity to the AcrAB transporter.

The checkerboard assays were not only carried out for *E. coli* BAA1161 but *E. coli* BW25113 was included in the study as well. However, no statistically significant decrease in the intrinsic MIC values of PIP or OFX in the presence of either EPI (see Appendix 6) was detected. On the other hand, it was quite unlikely that these ATB-EPI combinations would have shown to be synergistic because *E. coli* BW25113 was not resistant to PIP or OFX in the first place. In fact, *E. coli* BW25113 was sensitive to both ATBs (MICs of PIP and OFX were 8- to 64-fold lower than the MIC-breakpoint for being classified as sensitive, respectively). Additionally, *E. coli* BW25113 was one of the strains with the lowest efflux activity in the H33342 accumulation assays, which is in agreement with the findings made both in the antibacterial susceptibility testing and in the checkerboard assays. However, the inclusion of *E. coli* BW25113 in the experiments was justified as it formed the only pair of isogenic strains together with TolC-deleted mutant *E. coli* JW5503, thus enabling the assessment of the contribution of efflux activity in the obtained results.

Assessing the response of five EPIs in seven *E. coli* strains has a true value in respect of the research carried out so far in this topic. In the literature search, we could not come across with studies in which as many classes of EPIs for as many non-isogenic *E. coli* strains would have been studied as we did here. In the study carried out by Vidal-Aroca *et al.* (2009), four EPIs (CCCP, PAβN, NMP and mefloquine) were included in the ethidium bromide efflux study. However, the efflux inhibitory activity of these four EPIs were assessed only in one wild-type *E. coli* strain. There have been studies where several structural derivatives from one lead compound have been evaluated in terms of their efflux inhibitory activity (Bohnert *et al.*, 2016; Wang *et al.*, 2017) but as said, the uniqueness of our study stems from a high number of different classes of EPIs. Most studies were carried out with a wild-type *E. coli* strain, its genetically modified efflux-deficient derivatives and either clinical MDR isolates or genetically modified efflux-

overexpressors, but this selection of strains may be explained by the aims that differed from ours. Genotypic and phenotypic tests were usually chosen either to confirm that an MDR phenotype of clinical *E. coli* isolates was mediated by increased efflux activity or to assess efflux inhibitory activity of novel compounds in efflux-overexpressing *E. coli* strain (e.g. Bohnert and Kern, 2005; Kern *et al.*, 2006; Opperman *et al.*, 2014; Helaly *et al.*, 2016). In our study instead, wild-type pathogenic and non-pathogenic *E. coli* strains of clinical relevance were tested in order to identify a strain that was suitable to be used as a model strain in HTS of novel EPIs.

The most investigated EPIs in *E. coli* are CCCP and PAβN (e.g. Bohnert and Kern, 2005; Ohene-Agyei *et al.*, 2014; Opperman *et al.*, 2014). In contrast, there are fewer studies regarding the capability of NMP, mefloquine and thioridazine to potentiate the antibacterial activity of ATBs in efflux-overexpressing *E. coli* strains. Indeed, the efflux inhibitory activity of thioridazine has mostly been demonstrated in the strains other than *E. coli*, such as *Mycobacterium* (Rodrigues *et al.*, 2008; Coelho *et al.*, 2015). The inclusion of mefloquine in the antibacterial susceptibility testing and in the checkerboard assays was justified because mefloquine seemed to be the most potent EPI in the H33342 accumulation assays. Additionally, there is a small number of studies where the efflux inhibitory activity of mefloquine in *E. coli* was discussed and mefloquine has mainly been studied and used in malaria chemoprophylaxis (Schlagenhauf *et al.*, 2010). By starting the project with a larger number of *E. coli* strains, EPIs and ATBs, we could generate useful data regarding the efflux activities of seven tested *E. coli* strains and the potencies of five tested EPIs, eventually resulting in the optimal combination of all three factors. At the end, the inclusion of several *E. coli* strains, EPIs and ATBs seemed to be necessary as only one ATB–EPI combination in one *E. coli* strain showed synergism that was most likely explained by the pump inhibition and not by antibacterial activity of the EPI itself. In conclusion, we constructed a unique assay flow to meet the objectives defined in the beginning of the project.

For the future research perspectives, it would be interesting to study more the following aspects. Mefloquine at 16 μg/ml was chosen to be used as a positive control in HTS of novel EPIs even though mefloquine seemed to have unspecific modes of action at the

concentrations higher than 0.5 μg/ml. However, there are no molecular mechanistic studies regarding the pump inhibition nor characterized mefloquine–AcrAB co-crystal structures which would have revealed the essential residues for establishing mefloquine–AcrAB complexes. Higher intracellular H33342 accumulation compared to that measured for untreated *E. coli* JW5503 could also suggest that mefloquine has efflux inhibitory activity towards EP systems other than TolC-connected EPs. In fact, it would be beneficial to have an EPI which has affinity to several EP systems within the same or multiple MDR-superfamilies because some ATBs may be extruded via a broader range of different EPs. Thus, the susceptibility to broader spectrum of antibacterial agents could be restored and not only to the ATBs that are selectively pumped out via specific EP system. However, the assumption of mefloquine altering the OM permeability requires more studies to be confirmed. In addition, it would have been interesting to define the profiles of (over)expressed EPs and (down)regulated porins in each *E. coli* strain by RT-qPCR to get a more holistic view of the *E. coli* strains included in the experiments.

5 CONCLUSIONS

AMR has become a real public health threat worldwide and the actions against it should be taken. AcrAB-TolC EP system, a member of RND-superfamily, plays a major role in mediating MDR in *E. coli* as it is capable of extruding a broad range of structurally unrelated compounds, thus causing cross-resistance to several classes of ATBs. Instead of allocating resources in the research and development of novel broad-spectrum antibacterial agents with activity against GNB, the resistance to existing ATBs could be reversed by adjuvant therapy using EPIs. Consequently, intracellular concentrations of ATBs could be increased to the therapeutic levels, which would make ATBs effective against these MDR GNB again.

In this study we defined the optimal assay conditions and a positive control to be used in the future for HTS of novel EPIs. H33342 accumulation assay in conjunction with EPIs provides a quick, simple and cheap method to evaluate the contribution of efflux activity to the measured steady-state levels of H33342 accumulation and to discriminate between *E. coli* strains with low and high intrinsic efflux activities. *E. coli* BAA1161 resulted in

the highest median increase in the intracellular H33342 accumulation when combined with any of the five tested EPIs. Based on the results obtained from the H33342 accumulation assays and the checkerboard assays, enhanced efflux activity seemed to contribute to the decreased susceptibility of *E. coli* BAA1161 to PIP as a 16- to 32-fold decrease in the intrinsic MIC of PIP was detected after the addition of mefloquine and CCCP at the concentrations corresponding to half of their MICs. With mefloquine, observed synergism was very likely explained by the pump inhibition and not by the antibacterial activity of mefloquine itself. In contrast, the antibacterial activity of CCCP could not be excluded as a contributor to the synergism observed between PIP and CCCP. In principle, mefloquine does not fulfill all criteria set for ideal EPIs, i.e. the results obtained from the H33342 accumulation assay conducted in *E. coli* JW5503 indicated that mefloquine may have additional modes of action or affinity to several different EP systems. Further studies would be needed to confirm this hypothesis. However, the possibility for the existence of unspecific mechanisms of action should be taken into account in HTS when the responses of library compounds are compared to that of positive control established in our study.

In conclusion, the main objectives of the project, defining the optimal assay conditions (*E. coli* strain and ATB at specific concentration) and a positive control (EPI at specific concentration) to be used in HTS of novel EPIs, were met. The final endpoint was achieved by starting with seven *E. coli* strains, five EPIs and four ATBs, gradually narrowing down in the number of three factors and finally resulting in *E. coli* BAA1161 as a model strain, 16 μg/ml mefloquine as EPI and 256 μg/ml PIP as ATB.

6 REFERENCES

Alcalde-Rico, M., Hernando-Amado, S., Blanco, P. & Martínez, J. L. Multidrug efflux pumps at the crossroad between antibiotic resistance and bacterial virulence. *Front. Microbiol.* **7,** 1–14 (2016).

Amaral, L., Martins, A., Molnar, J., Kristiansen, J. E., Martins, M., Viveiros, M., Rodrigues, L., Spengler, G., Couto, I., Ramos, J., Dastidar, S., Fanning, S. McCusker, M. & Pagès, J. M. Phenothiazines, bacterial efflux pumps and targeting the macrophage for enhanced killing of intracellular XDRTB. *In Vivo (Brooklyn).* **24,** 409–424 (2010).

Amaral, L., Cerca, P., Spengler, G., Machado, L., Martins, A., Couto, I., Viveiros, M., Fanning, S. & Pagès, J. M. Ethidium bromide efflux by Salmonella: Modulation by metabolic energy, pH, ions and phenothiazines. *Int. J. Antimicrob. Agents* **38,** 140–145 (2011).

Amaral, L., Martins, A., Spengler, G. & Molnar, J. Efflux pumps of Gram-negative bacteria: What they do, how they do it, with what and how to deal with them. *Front. Pharmacol.* **4,** 1–11 (2014).

Anes, J., McCusker, M. P., Fanning, S. & Martins, M. The ins and outs of RND efflux pumps in Escherichia coli. *Front. Microbiol.* **6,** 1–14 (2015).

Baba, T., Takeshi, A., Hasegawa, M., Takai, Y., Okumura, Y., Baba, M., Datsenko, K. A., Tomita, M., Wanner, B. L. & Mori, H. Construction of *Escherichia coli* K-12 in-frame, single-gene knockout mutants: the Keio collection. *Mol. Syst. Biol.* **2**, 2006.0008 (2006).

Blair, J. M. A. & Piddock, L. J. V. How to measure export via bacterial multidrug resistance efflux pumps. *mBio* **7,** 1–6 (2016).

Bohnert, J. A. & Kern, W. V. Selected arylpiperazines are capable of reversing multidrug resistance in *Escherichia coli* overexpressing RND efflux pumps. *Antimicrob. Agents Chemother.* **49,** 849 (2005).

Bohnert, J. A., Schuster, S., Kern, W. V., Karcz, T., Olejarz, A., Kaczor, A., Handzlik, J. & Kiec-Kononowicz, K. Novel piperazine arylideneimidazolones inhibit the AcrAB-TolC pump in *Escherichia coli* and simultaneously act as a fluorescent membrane probes in a combined real-time influx and efflux assay. *Antimicrob. Agents Chemother.* **60**, 1974–1983 (2016).

Brown, R. E., Stancato F. A. & Wolfe A. D. The effects of Mefloqine on *Escherichia coli*. *Life Sciences.* **25**, 1857–1864 (1979).

Cha, H. J., Müller, R. T. & Pos, K. M. Switch-loop flexibility affects transport of large drugs by the promiscuous AcrB multidrug efflux transporter. *Antimicrob. Agents Chemother.* **58,** 4767–4772 (2014).

Chapman, J. S. & Georgopapdakou, N. H. Routes of quinolone permeation in *Escherichia coli*. *Antimicrob. Agents Chemother.* **32,** 438–442 (1988).

CLSI. Methods for Dilution Antimicrobial Susceptibility Tests for Bacteria That Grow Aerobically; Approved Standard—10th Edition. CLSI document M07-A10. Wayne, PA: Clinical and Laboratory Standards Institute (2015).

CLSI. Performance Standards for Antimicrobial Susceptibility Testing. 28th Edition. CLSI supplement M100. Wayne, PA: Clinical and Laboratory Standards Institute (2018).

Coelho, T., Machado, D., Couto, I., Maschmann, R., Ramos, D., von Groll, A., Rossetti, M. L., Silva, P. A. & Viveiros, M. Enhancement of antibiotic activity by efflux inhibitors against multidrug resistant *Mycobacterium tuberculosis* clinical isolates from Brazil. *Front. Microbiol.* **6,** 1–12 (2015).

Coldham, N. G., Webber, M., Woodward, M. J. & Piddock, L. J. V. A 96-well plate fluorescence assay for assessment of cellular permeability and active efflux in *Salmonella enterica serovar Typhimurium* and *Escherichia coli*. *J. Antimicrob. Chemother.* **65,** 1655–1663 (2010).

Danelon, C., Nestorovich, E. M., Winterhalter, M., Ceccarelli, M. & Bezrukov, S. M. Interaction of zwitterionic penicillins with the OmpF channel facilitates their translocation. *Biophys J.* **90**, 1617–1627 (2005).

Delcour, A. H. Outer membrane permeability and antibiotic resistance. *Biochim. Biophys. Acta.* **1794,** 808–816 (2009).

DrugBank (online). Ofloxacin. (Accessed: 1.12.2018). Available online: https://www.drugbank.ca/drugs/DB01165

DrugBank (online). Piperacillin Sodium. (Accessed: 1.12.2018). Available online: https://www.drugbank.ca/salts/DBSALT001067

Du, D., Wang, Z., James, N. R., Voss, J. E., Klimont, E., Ohene-Agyei, T., Venter, H., Chiu, W. & Luisi, B. F. Structure of the AcrAB-TolC multidrug efflux pump. *Nature* **509,** 512–515 (2014).

Eicher, T., Brandstätter, L. & Pos, K. M. Structural and functional aspects of the multidrug efflux pump AcrB. *Biol. Chem.* **390,** 693–699 (2009).

Eicher, T., Cha, H. J., Seeger, M. A., Brandstätter, L., El-Delik, J., Bohnert, J. A., Kern, W. V., Verrey, F., Grütter, M. G., Diederichs, K. & Pos, K. M. Transport of drugs by the multidrug transporter AcrB involves an access and a deep binding pocket that are separated by a switch-loop. *Proc. Natl. Acad. Sci.* **109,** 5687–5692 (2012).

Eswaran, J., Koronakis, E., Higgins, M. K., Hughes, C. & Koronakis, V. Three's company: Component structures bring a closer view of tripartite drug efflux pumps. *Curr. Opin. Struct. Biol.* **14,** 741–747 (2004).

Farha, M. A., Verschoor, C. P., Bowdish, D. & Brown, E. D. Collapsing the proton motive force to identify synergistic combinations against *Staphylococcus aureus*. *Chem. Biol.* **20**, 1168–1178 (2013).

Helaly, G. F., Shawky, S., Amer, R., Abdel-Kader, O., El-Sawaf, G. & El Kohy, M. A. Expression of AcrAB efflux pump and role of mefloquine as efflux pump inhibitor in MDR *E. coli*. *Am. J. Infect. Dis. Microbiol.* **4**, 6–13 (2016).

Hirai, K., Aoyama, H., Irikura, T., Iyobe, S. & Mitsuhashi, S. Differences in susceptibility to quinolones of outer membrane mutants of *Salmonella typhimurium* and *Escherichia coli*. *Antimicrob. Agents Chemother.* **29,** 535–538 (1986).

Hirakata, Y., Srikumar, R., Poole, K., Gotoh, N., Suematsu, T., Kohno, S., Kamihira, S., Hancock, R. E. & Speert, D. P. Multidrug efflux systems play an important role in the invasiveness of *Pseudomonas aeruginosa*. *J. Exp. Med.* **196,** 109–118 (2002).

Hirakata, Y., Kondo, A., Hoshino, K., Yano, H., Arai, K., Hirotani, A., Kunishima, H., Yamamoto, N., Hatta, M., Kitagawa, M., Kohno, S. & Kaku, M. Efflux pump inhibitors reduce the invasiveness of *Pseudomonas aeruginosa*. *Int. J. Antimicrob. Agents.* **34,** 343–346 (2009).

Iino, R., Nishino, K., Noji, H., Yamaguchi, A. & Matsumoto, Y. A microfluidic device for simple and rapid evaluation of multidrug efflux pump inhibitors. *Front. Microbiol.* **3,** 1–9 (2012).

Inglese, J., Johnson, R. L., Simeonov, A., Xia, M., Zheng, W., Austin, C. P. & Auld, D. S. High-thoughput screening assays for the identification of chemical probes. *Nat. Chem. Biol.* **3**, 466–479 (2007).

Kadenbach, B. Intrinsic and extrinsic uncoupling of oxidative phosphorylation. *Biochim. Biophys. Acta - Bioenerg.* **1604,** 77–94 (2003).

Kern, W. V., Steinke, P., Schumacher, A., Schuster, S., von Baum, H. & Bohnert, J. A. Effect of 1-(1-naphthylmethyl)-piperazine, a novel putative efflux pump inhibitor, on antimicrobial drug susceptibility in clinical isolates of *Escherichia coli*. *J. Antimicrob. Chemother.* **57,** 339–343 (2006).

Kinoshita, N., Unemoto, T. & Kobayashi, H. Proton motive force is not obligatory for growth of *Escherichia coli*. **160,** 1074–1077 (1984).

Koronakis, V., Sharff, A., Koronakis, E., Luisi, B. & Hughes, C. Crystal structure of the bacterial membrane protein TolC central to multidrug efflux and protein export. *Nature* **405,** 914–919 (2000).

Krishnamoorthy, G., Tikhonova, E. B. & Zgurskaya, H. I. Fitting periplasmic membrane fusion proteins to inner membrane transporters: Mutations that enable *Escherichia coli* AcrA to function with *Pseudomonas aeruginosa* MexB. *J. Bacteriol.* **190,** 691–698 (2008).

Kumar, S. & Varela, M. F. Molecular mechanisms of bacterial resistance to antimicrobial agents. Microbial pathogens and strategies for combating them: science, technology and education (A. Méndez-Vilas, Ed.) *Formatex*, 522–534 (2013).

Kunin, C. M. & Ellis, W. Y. Antimicrobial activities of mefloquine and a series of related compounds. **44,** 848–852 (2000).

Lamers, R. P., Cavallari, J. F. & Burrows, L. L. The efflux inhibitor phenylalanine-arginine beta-naphthylamide (PAβN) permeabilizes the outer membrane of Gram-negative bacteria. *PLoS One* **8,** 1–7 (2013).

Levine, M. M., Berquist, E. J., Nalin, D. R., Waterman, D. H., Hornich, R. B., Young, C. R. & Sotman, S. *Escherichia coli* strains that cause diarrhea but do not produce heat-labile or heat-stable enterotoxins and are non-invasive. *Lancet* **1**, 1119–1122 (1978).

Li X.Z. & Nikaido, H. Efflux-mediated drug resistance in bacteria. *Drugs* **64,** 159–204 (2004).

Lim, S. P. & Nikaido, H. Kinetic parameters of efflux of penicillins by the multidrug efflux transporter AcrAB-TolC of *Escherichia coli*. *Antimicrob. Agents Chemother.* **54**, 1800–1806 (2010).

Lomovskaya, O., Warren, M. S., Lee, A., Galazzo, J., Fronko, R., Lee, M., Blais, J., Cho, D., Chamberland, S., Renau, T., Leger, R., Hecker, S., Watkins, W., Hoshino, K., Ishida, H. & Lee, V. J. Identification and characterization of inhibitors of multidrug resistance efflux pumps in *Pseudomonas aeruginosa*: Novel agents for combination therapy identification and characterization of inhibitors of multidrug resistance efflux pumps in *Pseudomonas aeruginosa*. *Antimicrob. Agents Chemother.* **45,** 105–116 (2001).

Mahamoud, A., Chevalier, J., Alibert-Franco, S., Kern, W. V. & Pagès, J. M. Antibiotic efflux pumps in Gram-negative bacteria: The inhibitor response strategy. *J. Antimicrob. Chemother.* **59,** 1223–1229 (2007).

Manges, A. R., Tabor, H., Tellis, P., Vincent, C. & Tellier, P-P. Endemic and epidemic lineages of *Escherichia coli* that cause urinary tract infections. *Emerg. Infect. Dis.* **14**, 1575–1583 (2008).

Martins, A., Machado, L., Costa, S., Cerca, P., Spengler, G., Viveiros, M. & Amaral, L. Role of calcium in the efflux system of *Escherichia coli*. *Int. J. Antimicrob. Agents* **37,** 410–414 (2011).

Matsumoto, Y., Hayama. K., Sakakihara, S., Nishino, K., Noji, H., Iino, R. & Yamaguchi, A. Evaluation of multidrug efflux pump inhibitors by a new method using microfluidic channels. *PLoS One* **6,** 1–12 (2011).

Mesaros, N., Glupczynski, Y., Avrain, L., Caceres, N. E., Tulkens, P. M. & Bambeke, F. A combined phenotypic and genotypic method for the detection of Mex efflux pumps in *Pseudomonas aeruginosa*. *J. Antimicrob. Chemother.* **59**, 378–386 (2007).

Misra, R., Morrison, K. D., Cho, H. J. & Khuu, T. Importance of real-time assays to distinguish multidrug efflux pump-inhibiting and outer membrane-destabilizing activities in *Escherichia coli*. *J. Bacteriol.* **197,** 2479–2488 (2015).

Mojsoska, B. & Jenssen, H. Peptides and peptidomimetics for antimicrobial drug design. *Pharmaceuticals* **8,** 366–415 (2015).

Murakami, S., Nakashima, R., Yamashita, E., Matsumoto, T. & Yamaguchi, A. Crystal structures of a multidrug transporter reveal a functionally rotating mechanism. *Nature* **443,** 173–179 (2006).

Murakami, S. Multidrug efflux transporter, AcrB-the pumping mechanism. *Curr. Opin. Struct. Biol.* **18,** 459–465 (2008).

Nakashima, R., Sakurai, K., Yamasaki, S., Nishino, K. & Yamaguchi, A. Structures of the multidrug exporter AcrB reveal a proximal multisite drug-binding pocket. *Nature* **480,** 565–569 (2011).

Nakashima, R., Sakurai, K., Yamasaki, S., Hayashi, K., Nagata, C., Hoshino, K., Onodera, Y., Nishino, K. & Yamaguchi, A. Structural basis for the inhibition of bacterial multidrug exporters. *Nature* **500,** 102–106 (2013).

Naseem, R., Wann, K. T., Holland, I. B. & Campbell, A. K. ATP regulates calcium Efflux and growth in *E. coli*. *J. Mol. Biol.* **391,** 42–56 (2009).

Nikaido, H., Basina, M., Nguyen, V. Y. & Rosenberg, E. Y. Multidrug efflux pump AcrAB of *Salmonella Typhimurium* excretes only those β-lactam antibiotics containing lipophilic side chains. *J. Bacteriol.* **180**, 4686–4692 (1998).

Nikaido, H. Molecular basis of bacterial outer membrane permeability revisited. *Microbiol. Mol. Biol. Rev.* **67**, 593–656 (2003).

Nishino, K., Nikaido, E. & Yamaguchi, A. Regulation and physiological function of multidrug efflux pumps in *Escherichia coli* and S*almonella*. *Biochim. Biophys. Acta - Proteins Proteomics* **1794,** 834–843 (2009).

Oethinger, M., Kern, W. V., Jellen-Ritter, A. S., McMurry, L. M. & Levy, S. B. Ineffectiveness of topoisomerase mutations in mediating clinically significant fluoroquinolone resistance in *Escherichia coli* in the absence of the AcrAB efflux pump. *Antimicrob. Agents. Chemother.* **44**, 10–13 (2000).

Ohene-Agyei, T., Mowla, R., Rahman, T. & Venter, H. Phytochemicals increase the antibacterial activity of antibiotics by acting on a drug efflux pump. *Microbiologyopen* **3,** 885–896 (2014).

Opperman, T. J., Kwasny, S. M., Kim, H. S., Nguyen, S. T., Houseweart, C., D'Souza, S., Walker, G. C., Peet, N. P., Nikaido, H. & Bowlin, T. L. Characterization of a novel pyranopyridine inhibitor of the AcrAB efflux pump of *Escherichia coli*. *Antimicrob. Agents Chemother.* **58,** 722–733 (2014).

Opperman, T. J. & Nguyen, S. T. Recent advances toward a molecular mechanism of efflux pump inhibition. *Front. Microbiol.* **6,** 1–16 (2015).

Padilla, E., Llobet, E., Doménech-Sánchez, A., Martínez-Martínez, L., Bengoechea, J. A. & Albertí, S. *Klebsiella pneumoniae* AcrAB efflux pump contributes to antimicrobial resistance and virulence. *Antimicrob. Agents Chemother.* **54,** 177–183 (2010).

Pagès, J. M., James, C. E. & Winterhalter, M. The porin and the permeating antibiotic: A selective diffusion barrier in Gram-negative bacteria. *Nat. Rev. Microbiol.* **6,** 893–903 (2008).

Pagès, J. M. & Amaral, L. Mechanisms of drug efflux and strategies to combat them: Challenging the pump of Gram-negative bacteria. *Biochim. Biophys. Acta.* **1794**, 826–833 (2009).

Pérez, A., Poza, M., Fernández, A., Fernández Mdel, C., Mallo, S., Merino, M., Rumbo-Feal, S., Cabral, M. P. & Bou, G. Involvement of the AcrAB-TolC efflux pump in the resistance, fitness, and virulence of *Enterobacter cloacae*. *Antimicrob. Agents Chemother.* **56,** 2084–2090 (2012).

Piddock, L. J. Multi-drug resistance efflux pumps – not just for resistance. *Nat. Rev. Microbiol.* **4**, 629–636 (2006).

Piers, K. L. & Hancock, R. E. W. The interaction of a recombinant cecropin/melittin hybrid peptide with the outer membrane of *Pseudomonas aeruginosa*. *Mol. Microbiol.* **12,** 951–958 (1994).

Richmond, G. E., Chua, K. L. & Piddock, L. J. V. Efflux in *Acinetobacter baumannii* can be determined by measuring accumulation of H33342 (bis-benzamide). *J. Antimicrob. Chemother.* **68,** 1594–1600 (2013).

Rodrigues, L., Wagner, D., Viveiros, M., Sampaio, D., Couto, I., Vavra, M., Kern, W. V. & Amaral, L. Thioridazine and chlorpromazine inhibition of ethidium bromide efflux in *Mycobacterium avium* and *Mycobacterium smegmatis*. *J. Antimicrob. Chemother.* **61,** 1076–1082 (2008).

Sawyer, J. G., Martin, N. L. & Hancock, R. E. W. Interaction of macrophage cationic proteins with the outer membrane of *Pseudomonas aeruginosa*. *Infect. Immun.* **56,** 693–698 (1988).

Schlagenhauf, P., Adamcova, M., Regep, L., Schaerer, M. T. & Rhein, H-G. The position of mefloquine as a 21st centrury malaria chemoprophylaxis. *Malar. J.* **9**:357 (2010).

Schumacher, A., Steinke, P., Bohnert, J. A., Akova, M., Jonas, D. & Kern, W. V. Effect of 1-(1-naphthylmethyl)-piperazine, a novel putative efflux pump inhibitor, on antimicrobial drug susceptibility in clinical isolates of *Enterobacteriaceae* other than *Escherichia coli*. *J. Antimicrob. Chemother.* **57,** 344–348 (2006).

Schuster, S., Kohler, S., Buck, A., Dambacher, C., König, A., Bohnert, J. A. & Kern, W. V. Random mutagenesis of the multidrug transporter AcrB from *Escherichia coli* for identification of putative target residues of efflux pump inhibitors. *Antimicrob. Agents Chemother.* **58,** 6870–6878 (2014).

Seeger, M. A., Schiefner, A., Eicher, T., Verrey, F., Diederichs, K. & Pos, K. M. Structural Asymmetry of AcrB timer suggests a peristaltic pump mechanism. *Science* **313,** 1295–1298 (2006).

Seigel, G. M. & Campbell, L. M. High-throughput microtiter assay for Hoechst 33342 dye uptake. *Cytotechnology* **45**, 155–160 (2004).

Sekyere, J. O. & Amoako, D. G. Carbonyl cyanide m-chlorophenylhydrazine (CCCP) reverses resistance to colistin, but not to Carbapenems and tigecycline in multidrug-resistant *Enterobacteriaceae*. *Front. Microbiol.* **8,** 228 (2017).

Silhavy, T., Kahne, D. & Walker, S. The bacterial cell envelope. *Cold Spring Harb. Perspect. Biol.* **2,** 1–16 (2010).

Simonet, V., Malléa, M. & Pagès, J. M. Substitutions in the eyelet region disrupt cefepime diffusion through the *Escherichia coli* OmpF channel. *Antimicrob. Agents. Chemother.* **44**, 311–315 (2000).

Sinha, D., Pandey, S., Singh, R., Tiwari, V., Sad, K. & Tandon, V. Synergistic efficacy of bisbenzimidazole and carbonyl cyanide 3-chlorophenylhydrazone combination against MDR bacterial strains. *Sci. Rep.* **7**, 44419 (2017).

Sulavik, M. C., Houseweart, C., Cramer, C., Jiwani, N., Murgolo, N., Greene, J., DiDomenico, B., Shaw, K. J., Miller, G. H., Hare, R. & Shimer, G. Antibiotic susceptibility profiles of *Escherichia coli* strains lacking multidrug efflux pump genes. *Antimicrob. Agents Chemother.* **45,** 1126–36 (2001).

Terada, H. Uncouplers of oxidative phosphorylation. *Environ. Health. Perspect.* **87**, 213–218 (1990).

Thanassi, D. G., Cheng, L. W. & Nikaido, H. Active efflux of bile salts by *Escherichia coli*. *J. Bacteriol.* **179**, 2512–2518 (1997).

Tommasi, R., Iyer, R. & Miller, A. A. Antibacterial drug discovery: some assembly required. *ACS Infect. Dis.* **4**, 686–695 (2018).

Tortora, G. J., Funke, B. R., Case, C. L. Microbial Growth. In book: Microbiology: An introduction. p. 190, Global Edition. 12th Edition. Pearson Education Limited (2016).

Vargiu, A. V., Ruggerone, P., Opperman, T. J., Nguyen, S. T. & Nikaido, H. Molecular mechanism of MBX2319 inhibition of *Escherichia coli* AcrB multidrug efflux pump and comparison with other inhibitors. *Antimicrob. Agents Chemother.* **58,** 6224–6234 (2014).

Venter, H., Mowla, R., Ohene-Agyei, T. & Ma, S. RND-type drug efflux pumps from Gram-negative bacteria: Molecular mechanism and inhibition. *Front. Microbiol.* **6,** 1–11 (2015).

Vidal-Aroca, F., Meng, A., Minz, T., Pagès, M. G. P. & Dreier, J. Use of resazurin to detect mefloquine as an efflux-pump inhibitor in *Pseudomonas aeruginosa* and *Escherichia coli*. *J. Microbiol. Methods* **79,** 232–237 (2009).

Viveiros, M., Jesus, A., Brito, M., Leandro, C., Martins, M., Ordway, D., Molnar, A. M., Molnar, J. & Amaral, L. Inducement and reversal of tetracycline resistance in *Escherichia coli* K-12 expression of proton gradient-dependent multidrug efflux pump genes. *Society* **49,** 3578–3582 (2005).

Ventola, C. L. The antibiotic resistance crisis, part 1: causes and threats. *PT.* **40**, 277–283 (2015).

Wang, Y., Mowla, R., Guo, L., Ogunniyi, A. D., Rahman, T., De Barros Lopes, M. A., Ma, S. & Venter, H. Evaluation of a series of 2-napthamide derivatives as inhibitors of the drug efflux pump AcrB for the reversal of antimicrobial resistance. *Bioorg. Med. Chem. Lett.* **27**, 733–739 (2017).

World Health Organization. Antimicrobial Resistance: Global Report on Surveillance. Geneva (2014).

World Health Organization. Global Antimicrobial Resistance Surveillance System (GLASS) Report: early Implementation 2016–2017. Geneva (2017a).

World Health Organization. Prioritization of pathogens to guide discovery, research and development of new antibiotics for drug resistant bacterial infections, including tuberculosis. WHO/EMP/IAU/2017.12. Geneva (2017b).

Yang, J-H., Gross, R. L., Basinger S. F. & Wu, S. M. Apoptotic cell death of cultured salamander photoreceptors induced by CCCP: CsA-insensitive mitochondrial permeability transition. *J. Cell. Sci.* **114**, 1655–16564 (2001).

Zhang, J-H., Chung, T. D. & Oldenburg, K. R. A simple statistical parameter for use in evaluation and validation of high throughput screening assays. *J. Biomol. Screen.* **4**, 67–73 (1999).

Zhou, Z., Li, X., Liu, M., Beutin, L., Xu, J., Ren, Y., Feng, L., Lan, R., Reeves, P. R. & Wang, L. Derivation of *Escherichia coli* O157:H7 from its O55:H7 precursor. *PLoS One.* **14**, e8700 (2010).

APPENDIX 1: Bacterial growth rates of seven *E. coli* strains

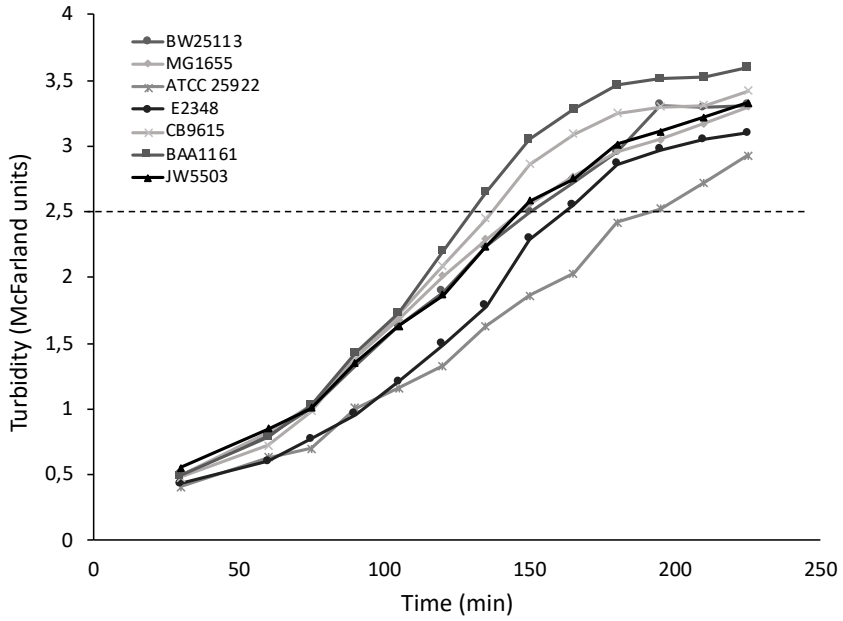

Figure 1. Results of one bacterial growth rate experiment. Overnight cultures of seven *E. coli* strains were inoculated into a fresh LB broth at a 1:100 dilution and the growth rates of *E. coli* strains were determined after 30 minutes of incubation at 37°C with shaking (200 rpm) by measuring the turbidity with the DEN-1 densitometer (Biosan). Measurements were taken at time points 30 and 60 minutes and thereafter every 15 minutes until the last time point 225 minutes. Between the measurements the cultures were incubated at 37°C with shaking (200 rpm). The threshold value of 2.5 McFarland units was achieved the fastest with *E. coli* BAA1161 and the slowest with E. *coli* ATCC 25922.

APPENDIX 2: Concentration ranges used in the MIC value determination

Table 1. Concentration ranges of ATBs and EPIs used in the MIC value determination. Unless otherwise stated, each concentration range was tested twice. The MIC Quality Control ranges for reference strain *E. coli* ATCC 25922 are shown in italics (CLSI, 2018).

Strain	CIP	OFX	TET	PIP	CCCP	Mefloquine
ATCC 25922	0.125 – 0.0625 – 0.0313 – *0.0156 – 0.0078 – 0.0039* – 0.002 – 0.001	0.48 – 0.24 – *0.12 – 0.06 – 0.03 – 0.015* – 0.0075 – 0.00375	16 – 8 – 4 – *2 – 1 – 0.5* – 0.25 – 0.125	32 – 16 – 8 – *4 – 2 – 1* – 0.5 – 0.25	80 – 40 – 20 – 10 – 5 – 2.5 – 1.25 – 0.625	32 – 16 – 8 – 4 – 2 – 1 – 0.5 – 0.25
BW25113	0.25 – 0.125 – 0.0625 – 0.0313 – 0.0156 – 0.0078 – 0.0039 – 0.002	0.96 – 0.48 – 0.24 – 0.12 – 0.06 – 0.03 – 0.015 – 0.0075	32 – 16 – 8 – 4 – 2 – 1 – 0.5 – 0.25 (x1) 16 – 8 – 4 – 2 – 1 – 0.5 – 0.25 – 0.125 (x3)[b]	64 – 32 – 16 – 8 – 4 – 2 – 1 – 0.5	10 – 5 – 2.5 – 1.25 – 0.625 – 0.313 – 0.156 – 0.078 (x1)[a] 80 – 40 – 20 – 10 – 5 – 2.5 – 1.25 – 0.625 (x3)[b]	32 – 16 – 8 – 4 – 2 – 1 – 0.5 – 0.25

Table 1. (*continued*)

Strain	CIP	OFX	TET	PIP	CCCP	Mefloquine
JW5503	0.125 – 0.0625 – 0.0313 – 0.0156 – 0.0078 – 0.0039 – 0.002 – 0.001	0.48 – 0.24 – 0.12 – 0.06 – 0.03 – 0.015 – 0.0075 – 0.00375 (x3)[b]	16 – 8 – 4 – 2 – 1 – 0.5 – 0.25 – 0.125	32 – 16 – 8 – 4 – 2 – 1 – 0.5 – 0.25 (x1)[c] 0.5 – 0.25 – 0.125 – 0.0625 – 0.0313 – 0.0156 – 0.0078 – 0.0039 (x2)	10 – 5 – 2.5 – 1.25 – 0.625 – 0.313 – 0.156 – 0.078	32 – 16 – 8 – 4 – 2 – 1 – 0.5 – 0.25
BAA1161	0.25 – 0.125 – 0.0625 – 0.0313 – 0.0156 – 0.0078 – 0.0039 – 0.002 (x3)[b]	0.96 – 0.48 – 0.24 – 0.12 – 0.06 – 0.03 – 0.015 – 0.0075	32 – 16 – 8 – 4 – 2 – 1 – 0.5 – 0.25 (x1)[a] 256 – 128 – 64 – 32 – 16 – 8 – 4 – 2 (x3)[b]	64 – 32 – 16 – 8 – 4 – 2 – 1 – 0.5 (x1)[a] 512 – 256 – 128 – 64 – 32 – 16 – 8 – 4 (x3)[b]	80 – 40 – 20 – 10 – 5 – 2.5 – 1.25 – 0.625	32 – 16 – 8 – 4 – 2 – 1 – 0.5 – 0.25

[a] This concentration range was tested only once because no inhibition was observed, in other words no concentration of ATB/EPI was able to inhibit the bacterial growth.
[b] Two first MIC assays gave a different MIC-value (one 2-fold difference) so the third assay was required to confirm which one was the correct MIC.
[c] This concentration range was tested only once because no bacterial growth was observed, in other words all concentrations of ATB/EPI could inhibit the bacterial growth.

APPENDIX 3: Optimization of Biomek i7 protocol

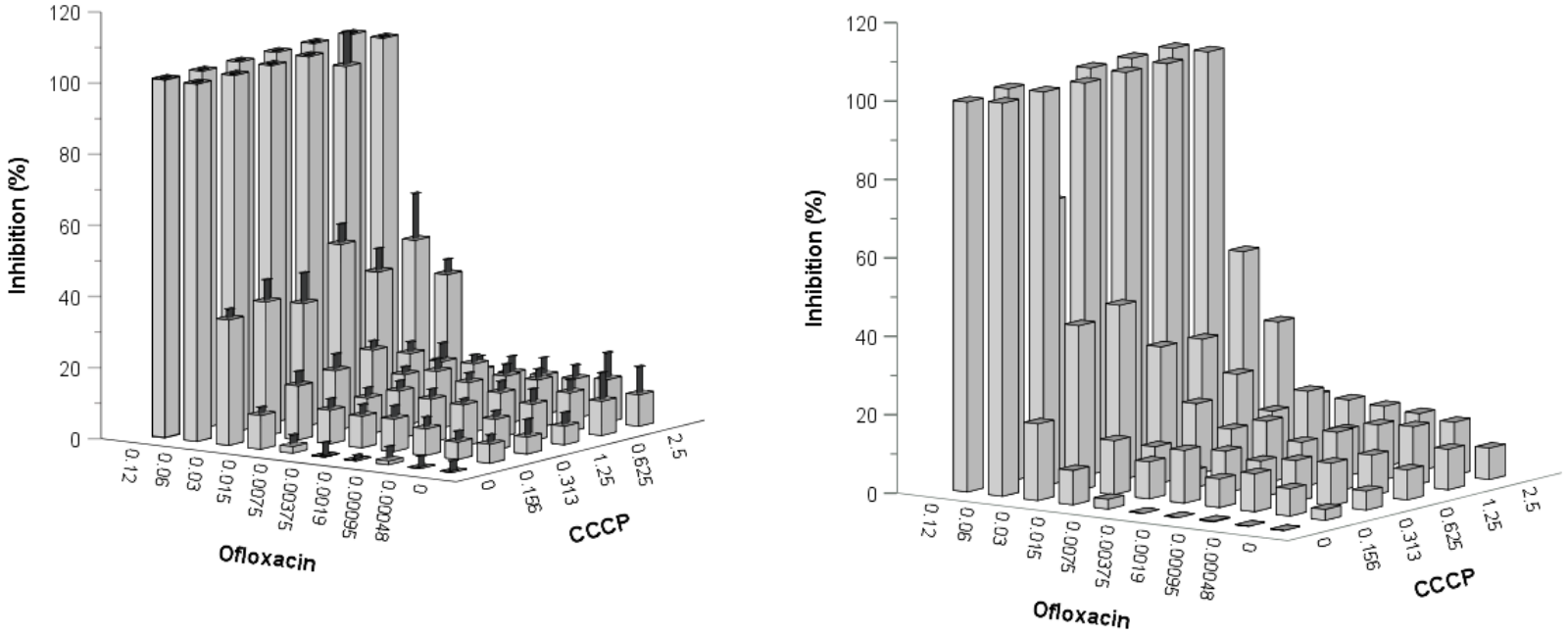

Figure 1. In the left figure the mean inhibition of three plates (run on the same day) ± SD are shown as 3D bars, each bar representing one well. In the right figure the results of the manual control plate are plotted. The similar trend along x- and z-axes is seen in both figures, concluding that the protocol optimization has succeeded. Relatively small plate-to-plate variation justify the continuation of the checkerboard assays only with one plate per run that is repeated twice, resulting in three separate runs for one ATB–EPI combination (day-to-day variation).

APPENDIX 4: Quality control parameters as a tool to define the optimal assay duration

Table 1. Quality parameters, Z', S/N and S/B, mostly used in the quality assessment of HTS assays were adopted here to determine the optimal assay duration for H33342 accumulation assay in the presence of EPIs. If higher values than 0.5 and 2-fold were obtained for Z'-factor and S/B, the assay was considered to be acceptable (Zhang *et al.*, 1999; Inglese *et al.*, 2007). At time point 30 minutes higher Z', S/N and S/B values were obtained than at time point 15 minutes, thus the results of H33342 accumulation assays were plotted after 30 minutes of incubation at 37°C.

A. $$Z' = 1 - \frac{3*SD_{15min} + 3*SD_{0min}}{AVG_{15min} - AVG_{0min}}$$

Compound	*E. coli* strain					
	BW25113	MG1655	ATCC 25922	E2348	CB9615	BAA1161
Without	0.36	0.03	0.60	0.61	0.45	-0.04
CCCP	0.64	0.61	0.53	0.78	0.75	0.63
PAβN	0.34	0.72	0.74	0.83	0.67	0.79
NMP	0.71	0.71	0.73	0.78	0.83	0.78
Mefloquine	0.74	0.81	0.75	0.83	0.79	0.73
Thioridazine	0.76	0.35	0.69	0.78	0.78	0.54

B. $$Z' = 1 - \frac{3*SD_{30min} + 3*SD_{0min}}{AVG_{30min} - AVG_{0min}}$$

Compound	*E. coli* strain					
	BW25113	MG1655	ATCC 25922	E2348	CB9615	BAA1161
Without	0.60	0.42	0.60	0.74	0.67	0.42
CCCP	0.67	0.69	0.52	0.75	0.74	0.63
PAβN	0.39	0.77	0.77	0.82	0.88	0.65
NMP	0.76	0.76	0.78	0.80	0.84	0.83
Mefloquine	0.77	0.86	0.75	0.83	0.78	0.74
Thioridazine	0.76	0.48	0.75	0.87	0.85	0.65

Table 1. (*continued*)

C. $S/N = \frac{AVG_{15min} - AVG_{0min}}{\sqrt{(SD_{15min})^2 + (SD_{0min})^2}}$

Compound	*E. coli* strain					
	BW25113	MG1655	ATCC 25922	E2348	CB9615	BAA1161
Without	6.7	4.2	10.3	10.0	9.2	4.1
CCCP	12.3	11.4	8.9	19.2	22.0	13.6
PAβN	6.12	15.0	17.7	24.9	12.0	19.2
NMP	14.7	14.6	15.7	18.7	25.2	20.7
Mefloquine	16.4	23.6	16.8	24.5	26.1	15.3
Thioridazine	25.3	7.4	16.1	16.2	18.6	16.5

D. $S/N = \frac{AVG_{30min} - AVG_{0min}}{\sqrt{(SD_{30min})^2 + (SD_{0min})^2}}$

Compound	*E. coli* strain					
	BW25113	MG1655	ATCC 25922	E2348	CB9615	BAA1161
Without	10.6	7.1	10.1	15.4	14.8	7.1
CCCP	13.5	13.4	8.4	17.0	19.8	12.4
PAβN	6.8	20.0	20.8	24.1	36.8	15.9
NMP	17.8	17.7	18.8	20.7	27.6	26.8
Mefloquine	18.8	30.9	16.5	24.3	27.9	15.2
Thioridazine	25.0	9.5	27.1	29.7	27.8	24.7

E. $S/B = \frac{AVG_{15min}}{AVG_{0min}}$

Compound	*E. coli* strain					
	BW25113	MG1655	ATCC 25922	E2348	CB9615	BAA1161
Without	2.4	2.0	3.8	3.5	4.5	2.5
CCCP	1.9	1.9	1.8	2.7	2.2	1.9
PAβN	1.3	2.1	2.7	2.7	4.8	2.9
NMP	1.7	2.0	2.5	2.6	2.8	2.3
Mefloquine	1.5	1.9	2.5	3.3	3.4	2.0
Thioridazine	2.1	2.2	3.2	4.8	3.2	2.6

F. $S/B = \frac{AVG_{30min}}{AVG_{0min}}$

Compound	*E. coli* strain					
	BW25113	MG1655	ATCC 25922	E2348	CB9615	BAA1161
Without	3.1	2.7	4.8	4.3	6.6	3.9
CCCP	1.9	2.0	1.7	2.6	2.1	1.9
PAβN	1.3	2.3	3.1	2.8	5.9	3.4
NMP	1.9	2.3	2.7	2.8	3.2	2.7
Mefloquine	1.6	2.2	2.7	3.4	3.9	2.1
Thioridazine	2.2	2.5	3.6	6.2	3.6	3.3

APPENDIX 5: Mefloquine at 0.5 μg/ml was not potent against wild-type pathogenic and non-pathogenic *E. coli* strains

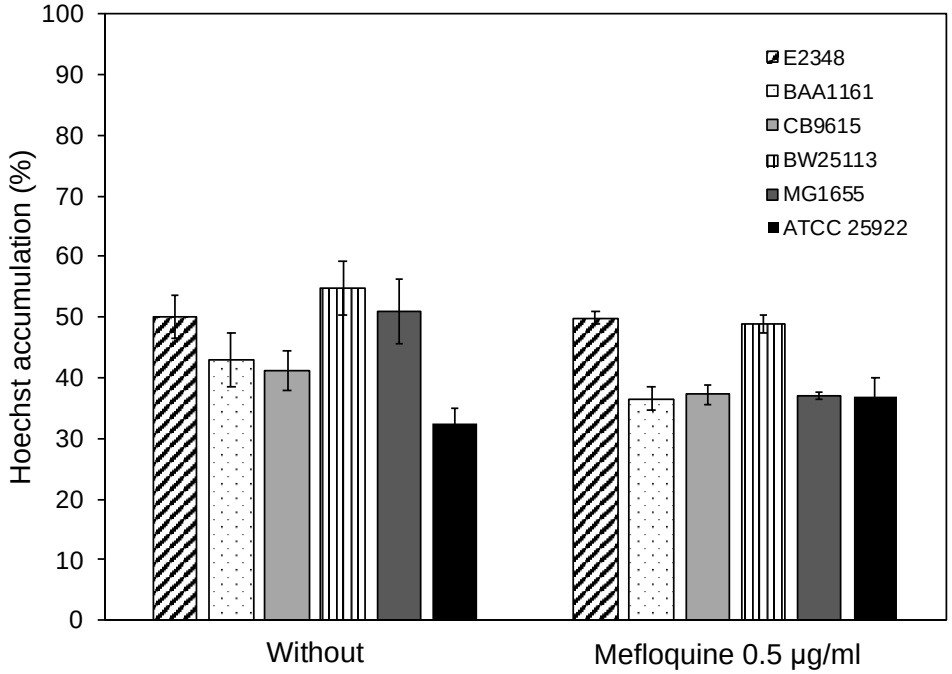

Figure 1. Steady-state levels of H33342 (2.5 μM) accumulation after 30 minutes of incubation at 37°C with mefloquine (0.5 μg/ml) in six *E. coli* strains. The results present the data of single assay (n = 8) ± SD and are plotted as a relative percentage of H33342 accumulation measured for untreated *E. coli* JW5503. The data obtained from H33342 accumulation assay assessing intrinsic efflux activities of *E. coli* strains was included in the same figure for comparison. In conclusion, six *E. coli* strains did not respond to mefloquine at 0.5 μg/ml. Thus, the assay was carried out only once and the concentration was increased up to 4, 8 and 16 μg/ml.

APPENDIX 6: Combinations of ATB and EPI that did not function synergistically

Figure 1. MICs of ATB in the presence of increasing concentrations of EPI are shown in a table and the inhibition of bacterial growth (%) is presented for each well of Nunc 96-well plate using colour-coding. The value in parentheses indicates the fold change relative to the intrinsic MIC value of ATB. The equations for modulation factor (MF) and fractional inhibitory concentration (FIC) has been provided in *Materials and methods* and the highest MF and the lowest FIC are shown in the table format adopted from Lomovskaya *et al.* (2001).

A.

Strain	Genotype	Mefloquine MIC (μg/ml)	OFX MIC (μg/ml) in the presence of Mefloquine at conc. (μg/ml) of						MF	FIC
			0	4	6	8	12	16		
BAA1161	UPEC	32	0.06	0.06 (1)	0.06 (1)	0.06 (1)	0.06 (1)	0.06 (1)	1	1

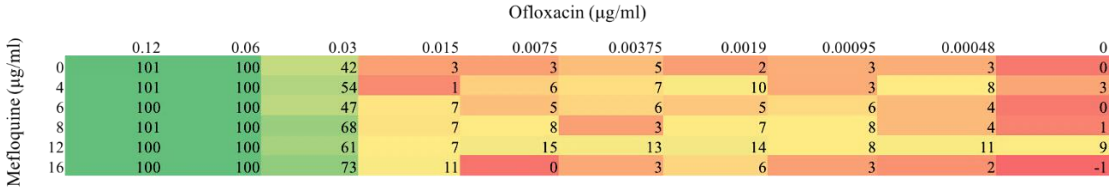

B.

Strain	Genotype	CCCP MIC (μg/ml)	OFX MIC (μg/ml) in the presence of Mefloquine at conc. (μg/ml) of						MF	FIC
			0	0.156	0.313	0.625	1.25	2.5		
BAA1161	UPEC	20	0.06	0.06 (1)	0.06 (1)	0.06 (1)	0.06 (1)	0.06 (1)	1	1

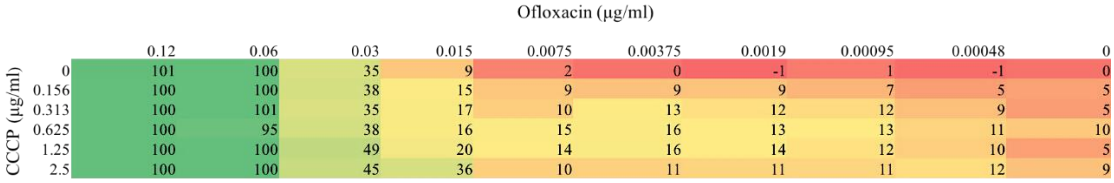

C.

Strain	Genotype	CCCP MIC (μg/ml)	PIP MIC (μg/ml) in the presence of CCCP at conc. (μg/ml) of						MF	FIC
			0	0.625	0.125	2.5	5	10		
BW25113	Wild-type	40	2	2 (1)	2 (1)	4[a]	4[a]	2 (1)	1	1

[a] Two outliers (the MIC of PIP should be 2.0 μg/ml)

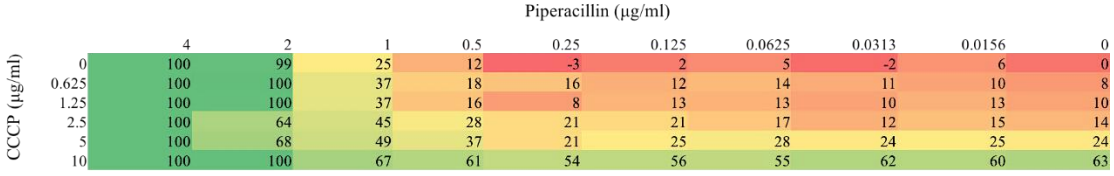

Figure 1. (*continued*)

D.

Strain	Genotype	CCCP MIC (μg/ml)	OFX MIC (μg/ml) in the presence of CCCP at conc. (μg/ml) of						MF	FIC
			0	0.156	0.313	0.625	1.25	2.5		
BW25113	Wild-type	40	0.06[a]	0.06 (1)	0.06 (1)	0.06 (1)	0.06 (1)	0.06 (1)	1	1

[a] Not the same MIC value determined in the antibacterial susceptibility testing (0.03 μg/ml)

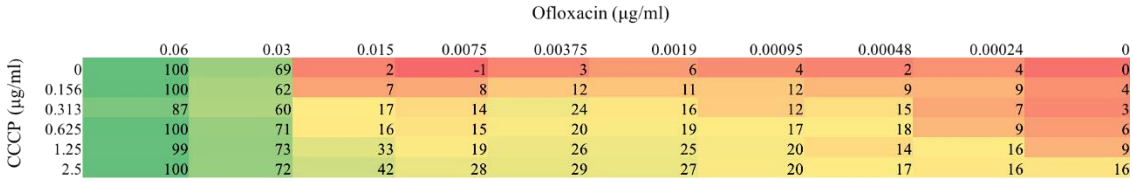

E.

Strain	Genotype	Mefloquine MIC (μg/ml)	PIP MIC (μg/ml) in the presence of Mefloquine at conc. (μg/ml) of						MF	FIC
			0	4	6	8	12	16		
BW25113	Wild-type	32	4[a]	4 (1)	4 (1)	4 (1)	4 (1)	2 (2)	2	0.5

[a] Not the same MIC value determined in the antibacterial susceptibility testing (2.0 μg/ml)

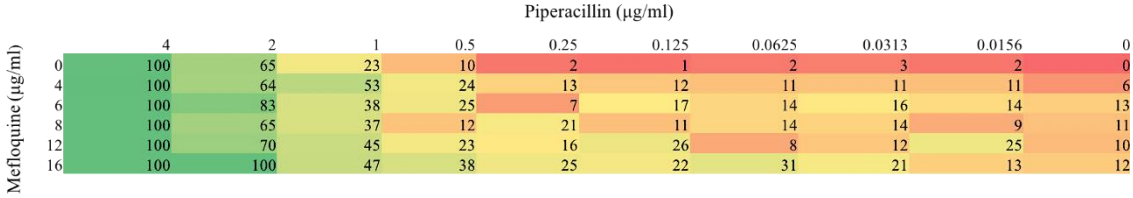

F.

Strain	Genotype	Mefloquine MIC (μg/ml)	OFX MIC (μg/ml) in the presence of Mefloquine at conc. (μg/ml) of						MF	FIC
			0	4	6	8	12	16		
BW25113	Wild-type	32	0.06[a]	0.06 (1)	0.06 (1)	0.06 (1)	0.06 (1)	0.06 (1)	1	1

[a] Not the same MIC value determined in the antibacterial susceptibility testing (0.03 μg/ml)